DNA-based construction at the nanoscale: Emerging trends and applications

P. Lourdu Xavier[1,2,*] and Arun Richard Chandrasekaran[3*]

[1] Center for Free Electron Laser Science, Deutsches Elektronen-Synchrotron (DESY) and Dept. of Physics, University of Hamburg, 22607 Hamburg, Germany.

[2] Max-Planck Institute for the Structure and Dynamics of Matter, Luruper Chaussee 149, 22761 Hamburg, Germany.

[3] Confer Health, Inc., Charlestown, Massachusetts, 02129, USA.

*Correspondence: lourdu-xavier.paulraj@mpsd.mpg.de (PLX) and arunrichard@nyu.edu (ARC)

Abstract

The field of structural DNA nanotechnology has evolved remarkably—from the creation of artificial immobile junctions to the recent DNA-protein hybrid nanoscale shapes—in a span of about 35 years. It is now possible to create complex DNA-based nanoscale shapes and large assemblies with greater stability and predictability, thanks to the development of computational tools and advances in experimental techniques. Although started with the original goal of DNA-assisted structure determination of difficult-to-crystallize molecules, DNA nanotechnology has found its applications in a myriad of fields. In this review, we cover some of the basic and emerging assembly principles: hybridization, base stacking/shape complementarity, and protein-mediated formation of nanoscale structures. We also review various applications of DNA nanostructures, with special emphasis on some of the biophysical applications that have been reported in recent years. In the outlook, we discuss further improvements in the assembly of such structures, and explore possible future applications involving super-resolved fluorescence, single-particle cryo-electron (cryo-EM) and X-ray free electron laser (XFEL) nanoscopic imaging techniques, and in creating new synergistic designer materials.

Keywords: DNA nanotechnology, DNA origami, DNA-protein hybrid, RNA, synthetic biology, photonics, plasmonics, structural biology, NMR, programmable matter, Cryo-EM, XFEL, super-resolution, fluorescence, high-speed atomic force microscopy (AFM), quantum imaging, ultra-fast, molecular scaffolds, single-particle imaging, molecular computation.

Outline

1. Introduction

Apart from being the genetic molecule, DNA is a viable material for the bottom-up construction of nanoscale shapes and structures [1–3]. Molecular recognition and self-assembly—the elegant principles of organization and function in living materials—are the driving forces behind the fabrication of DNA-based nanoscale materials. One of the foremost goals of nanotechnology is the creation of precisely programmed structures, through the control and manipulation of matter, comparable to those involved in biological processes [4]. Among the available bottom-up construction strategies [5, 6], DNA-based self-assembly has been remarkably effective in designing and building nanoscale objects [7]. Although other biomolecules such as proteins have been used for design and self-assembly, the process is complicated due to the availability of 20 amino acid building blocks and the complex interactions between them [8, 9]. DNA, with the four canonical nucleotides, provides a predictive self-assembly process based on the Watson–Crick base pairing (*simplicity in programmability*). The structural features of DNA form the basis of constructing a wide variety of architectures with well-defined shapes and sizes. For instance, the DNA duplex has a diameter of ~2 nm, a helical pitch of ~3.4–3.6 nm (*structurally repeating building block*), and a persistence length of ~50 nm (*rigidity for construction*). In addition, single-stranded overhangs called sticky ends can be used to connect duplexes providing a route to hierarchical assembly (*structural glue*). The better stability of DNA compared to other natural nucleic acids is another advantage for DNA to be a robust building block. DNA also provides flavor for construction at the nanoscale: for example, non-Watson–Crick base pairing (e.g. i-motifs, G-quadruplexes, triplexes) [10], protein binding (e.g. aptamers) [11], and enzymatic activity (e.g. DNAzymes) [12] provide additional tools for the creation of functional devices and machines. The field of DNA nanotechnology has expanded to find applications in areas such as chemistry, biology, computation, medicine, and materials science. In this article, we cover the basic and emerging principles for the fabrication of self-assembled DNA nanostructures and hierarchical assemblies and discuss some of their applications (See Figure 1 for an overview).

2. Assembly principles of self-assembled DNA nanostructures

The notion of using DNA to build structures was proposed by Seeman in the early 1980s [13]. The inherent nanoscale features of DNA (discussed above) allow it to be useful as a nanoscale building block. However, the DNA molecule is inherently linear and in order to achieve multi-dimensional assembly, branched DNA junctions are required. Inspired by Holliday junctions [14], Seeman synthesized specific DNA sequences and created an immobile four-arm DNA junction that can serve as a construction unit [15]. The number of arms around the junction can be expanded to contain 5, 6, 8 or 12 arms [16, 17]. Such crossover-based design of tiles or motifs have formed the basis of nanoscale construction using DNA, with higher order assembly provided by sticky ends (hybridization-based), shape complementarity or protein-mediated assembly.

2.1 Assembly based on hybridization

The first 3D objects created from DNA were a cube (Figure 2(A)) [18] and a truncated octahedron (Figure 2(B)) [19]. Assembly of such structures requires specific sequence design so that different regions of component DNA strands bind to their complementary regions in other strands. Another example is an octahedron built from a 1.7 kilobase DNA strand folded by five short strands (Figure 2(C)) [20]. Using a modular approach, icosahedral DNA structures have been constructed from pre-connected 5-arm DNA junctions (Figure 2(D)) [21]. A DNA tetrahedron constructed using four component strands is an example of designed assembly of component DNA strands without involving ligation and purification steps (Figures 2(E) and (F)) [22]. A DNA three- point-star motif has been used to create tetrahedra, dodecahedra, and buckyballs by controlling the flexibility and con- centration of the component tiles (Figure 2(G)) [23]. Each arm of the star-shaped DNA motif is a four-arm junction and can self-assemble into symmetric DNA polyhedra through sticky end hybridization. Furthermore, by controlling the symmetry of the three-point-star DNA motifs, a DNA cube has also been constructed (Figure 2(H)) [24]. Using a similar strategy, a five-point-star motif has been used to assemble an icosahedron (Figure 2(I)) [25]. In addition, 3D DNA prisms have been constructed using a stepwise strategy [26]. In this case, triangles or squares with rigid organic molecules at the vertices were first synthesized. Two such units were then connected by linking strands to create prism shapes (Figure 2(J)). A large number of DNA prismatic structures such as triangular, square, pentagonal, and hexagonal prisms were generated using this modular approach. Such DNA objects provide encapsulation and release of drugs and nanomaterials, control over activity of encapsulated proteins, for biosensing, and for the construction of 3D networks for catalysis [27].

The original goal of assembling materials with DNA was to build a 3D DNA scaffold that could host external guests for crystallization [13, 28]. In the process of achieving this goal, a variety of DNA motifs have been created and used for the construction of 2D arrays (Figure 3). Some examples of such DNA motifs are the double crossover (DX) [29] and the triple-crossover (TX) motifs [30] that have been used for the construction of well-defined 2D lattices with predesigned periodicity. Another type of motif, the paranemic crossover (PX) DNA [31] has been used to link topologically closed molecules and to create covalently linked 1D DNA arrays [32, 33]. A variety of other DNA motifs have also been developed for the construction of nanoscale objects and lattices [34]. Such 2D arrays are useful as programmable scaffolds for the organization of nanoparticles [35] and biomolecules [36], and their design, construction and applications have been reviewed before [37, 38]. Seeman and coworkers used a tensegrity triangle motif to create the first rationally designed 3D DNA crystal (Figure 4) [39]. The tensegrity triangle motif contains three double helical edges connected at the vertices by four arm junctions [40]. The ends of the helices are tailed with sticky ends so one triangle can connect to six such triangles. This assembly continues infinitely in three directions leading to the formation of an infinite periodic lattice (i.e. a crystal). Crystals with varying cavity sizes were also constructed by varying the edge length of these motifs [39, 41]. Moreover, the 3D self-assembly can be designed to contain two different asymmetric units [42], demonstrating the programmability of such an assembly. Crystals from the two-helical turn tensegrity triangle motif diffracted to 4 Å, and for it to be useful as a scaffold for macromolecular structure determination of external guests, the

robustness has to be improved (i.e. yield high resolution crystal structures). For this purpose, stability of such crystals were improved by biological production of component strands [43], sticky end modifications and sequence choice [44], triplex-reinforced sticky ends [45] and triplex-directed photo-crosslinking of the component motifs [46]. The role of heterogeneity and Watson–Crick interaction strengths in the growth of such crystals were also studied recently [47]. These designed DNA crystals have been used to host triplex-forming oligonucleotides that can tether external molecules on to the framework [48], a polyaniline molecule with potential in nanoelectronics [49], a color changing strand displacement-based device [50] and as a system to study torsionally stressed DNA with induced changes in the helical twist of the component motif [51].

Another strategy to build DNA nanostructures is to fold a long single stranded scaffold DNA (ssDNA) by hundreds of short complementary staple strands, a method known as DNA origami (Figure 5(A)) [52]. A precursor to the DNA origami concept is the octahedron built from a 1.7 kilobase DNA strand folded by five short strands [20]. While DNA origami was initially used for creating planar structures, the method was soon extended to first include the construction of 3D multilayer structures and then twisted 3D multilayer structures [53], twisted bundles [54], and hollow 3D structures such as boxes [55], spheres and flasks [56]. Moreover, wireframe and mesh-like architectures have also been created using DNA origami by designing specific folding patterns for the scaffold strand [57, 58]. Some examples of DNA origami structures are shown in Figures 5(B)–(G). The main advantages of the DNA origami strategy are the simplicity of using a singular scaffold strand and folding it into any desired shape, and the fact that it does not require purification or a stoichiometric mixture of component strands. By designing cross-shaped origami structures to contain sticky ends, long range two-dimensional arrays of DNA origami have been created (Figure 5(H)) [59]. In addition, origami structures containing sticky ends can also be hierarchically assembled into larger objects [60]. The strategies involved in the creation of origami structures and their applications were recently covered in a review by Hao Yan and colleagues [61]. Alternative approaches to DNA-based construction are the molecular canvas strategy (Figure 6(A)) [62] and assembly using DNA bricks (Figure 6(B)) [63]. These strategies are based on single stranded DNA tiles [64] containing four domains (shown in Figure 6(A)). Adjacent DNA single stranded tiles connect to each other by pairing up with complementary domains, and continue to form DNA lattices composed of parallel DNA helices.

2.2 Non-base pairing and shape-complementarity based self-assembly

Although Watson–Crick base-pairing is exceptionally powerful in creating self-assembled DNA nanostructures, non- base pairing interactions have also been exploited for the self-assembly of pre-formed DNA-motifs/nanostructures. Various weak interactions have been used to assemble materials: DNA/RNA-like multiple hydrogen bonds in heteroaromatic modules [65], π–π stacking [66, 67], capillary forces [68], and roughness-controlled depletion attractions (entropy depletion) [69]. In a sense, in the overall process of structure and organization of DNA, the roles of geometric stacking and base-pairing based hybridization are inseparable—where the main distinction is the specificity offered by hybridization. Though the role of stacking behavior in duplex DNA is well known [70], its implications in DNA nanotechnology have been

realized only of late. Blunt-end stacking of bent triple crossover motifs have been shown to result in 1D arrays [71]. However, these interactions produced an arbitrary assembly of the motifs with no specific periodicity when compared to those assembled using motifs containing sticky ends. In most assembly strategies, preventive steps are taken to avoid such stacking by choosing appropriate sequence design and by the addition of poly-T loops at blunt- end locations. However, stacking interactions have now been used to assemble pre-formed DNA motifs and structures, though less frequently than the hybridization-based method (involving sticky end connections). For example, blunt end stacking (homophilic attraction) and shape complementarity have been used in the hierarchical assembly of 2D DNA origami structures [72]. Geometric arrangement of stacked blunt ends can follow two approaches. The first approach encodes bond type using a 16 bit (strands) binary code along the edges of a 2D DNA origami rectangle (Figure 7(A)-(i)). By addition of specific staple strands, the edges of the rec- tangle can be programmed to end in blunt helices ('1') or by leaving out staples, these can be left as single stranded loops ('0'). Only the blunt helices allow stacking of adjacent rec- tangles. This is reprogrammable—for e.g. a single set of 16 strands can create 216 = 65536 bond types. The second approach encodes bond type using geometric complementarity between pairs of edge shapes; this approach is not reprogrammable—the shape complementarity is unique for a pair of origami structures (Figure 7(A)-(ii)). Symmetry of the structures, mismatch constraints and the flexibility of edges limit the number of usable bonds in such a system. One other limitation is that the total binding energy is limited by the size of the origami while in hybridization-based assembly, the binding energies can be tailored by varying the length of sticky ends. The principles of base-stacking have been extended to assemble discrete multilayer DNA origami objects that assemble in solution through shape complementarity to form various homo- and hetero-multimeric objects [73]. These objects were used in creating micrometer- scale assemblies and reconfigurable nanodevices such as actuators, switchable gears and a nanorobot (Figure 7(B)). The stability and functionality of these devices and assemblies could be controlled by cation concentration and temperature. Recently, an origami version of the tensegrity triangle was used to assemble designer 3D crystals, but instead of sticky ends connecting the units, this system relied on shape complementary blunt ends [74]. Surface-assisted assembly of 2D lattices can be achieved by close-packing of symmetric, non-interacting DNA origami structures, or by utilizing blunt-end stacking interactions between the origami units [75]. Adsorption of DNA origami structures on mica surface is mediated by Mg2+ ions, which act as salt bridges between mica and DNA. Addition of monovalent ions (such as Na+) partly replaces the Mg2+ ions and forms a more diffuse charge layer between the surface and the DNA [76]. As a result, the origami structures become mobile on the surface and can then associate to form extended, ordered structures on the surface (Figure 7(C)). Similar assembly of DNA lattices has been shown on lipid membranes. For example, blunt-ended DNA origami structures absorbed onto mica-supported lipid bilayers in the presence of divalent cations can associate to form ordered superstructures on the surface [77]. The bilayer-adsorbed origami units are mobile on the surface and self-assemble into large micro- meter-sized 2D lattices (Figure 7(D)).

2.3 Protein-mediated programmable assembly of DNA-protein hybrid nanoscale shapes

While assembling/patterning of proteins on preformed-DNA nanostructures have been prevalent, there are very few examples of protein-mediated assembly of DNA nanostructures and protein–nucleic acid hybrid nanomaterials. One example is a protein–DNA co-assembling strategy to create a hybrid nanowire [78]. A homodimerization interface was engineered onto the Drosophila Engrailed Homeodomain (ENH) that allowed the dimerized protein complex to bind to two double-stranded DNA (dsDNA) molecules. The protein binding sites on the dsDNA molecules were tailored to result in a nanowire formation (Figure 8(A)). The mechanism of formation of these hybrid structures was confirmed by x-ray crystallography. However, programmability is yet to be demonstrated in this method. A recent highlight is the work of Dietz and his colleagues where they used a set of transcription activator-like (TAL) effector proteins to induce folding of dsDNA to form DNA–protein nanoscale shapes (Figure 8(B)) [79]. Even though genetic encoding of DNA nanostructures has been reported earlier [80], the key idea here is that proteins act as analogs of oligonucleotide staples in ssDNA-based origami [52]. TAL effector protein-based folding of dsDNA scaffold was used to create various 3D nanoscale shapes even at constant room temperature (Figures 8(B)-(i)–(iv)). This method also has implications in improving our understanding of how compaction and organization of chromosomes work in biological conditions and protein-binding induced curvature in multilayer dsDNA-origami structures.

2.4 Computational tools for assembly design and analysis

Advances in a field are greatly influenced by the parallel development of key methods/techniques. To construct DNA nanostructures based on the assembly principles mentioned above, computational tools and efficient experimental designs have been developed in parallel. Computational tools have been of great use in structural design, prediction, and stability validation of artificial macromolecular structures and assemblies. Starting with Seeman's JUNKART [81] DNA nanotechnology has benefitted from the development of computational tools such as SEQUIN [82] and UNIQUIMER [83] for sequence symmetry minimization of oligonucleotides used in constructing DNA complexes. Modeling programs such as GIDEON [84], TIAMAT [85] and UNIQUIMER 3D [86] allow the design, visualization and analysis of DNA motifs and structures. The program caDNAno [87] is widely used for designing DNA origami structures and the interface DAEDALUS [88] can be used to convert any 3D solid object specified using a computer-aided design file into the synthetic DNA sequences required to synthesize the target object. The program CanDo [89] is used for predicting the solution shape and structure of designed DNA nanostructures. While such software are made available as end-user programs for designing DNA nanostructures, several other codes and algorithms used for this purpose might also be available in the public domain. Some of these developments were the fruits of the convergence of the then-ongoing efforts on molecular (DNA) computation and designing topological structures out of DNA. Furthermore, molecular dynamics tools have also been created to simulate DNA origami assembly processes [90, 91]. Recent reports have shown prediction and analysis of structural and mechanical aspects of both tile- and origami-based DNA nanostructures [92–94]. The assembly principles aided by computational and experimental advances

have led to the creation of a variety of intricate nanoscale DNA structures with applications ranging from mimicking biological nanomachines to new materials for sensing and imaging.

3. Applications

Myriad intriguing applications have been reported using DNA nanostructures and some of these have already been reviewed extensively. These include drug-delivery [95–102], biosensing [103–108], protein functionalization, scaffolding and enzyme cascades [38, 95, 109–111]. We discuss here recent applications of DNA-based self-assembled structures in the context of structural biophysics, molecular scaffolding, plasmonics/photonics and fluorescence imaging.

3.1 DNA-assisted molecular and structural biophysics

Hybridization, biochemical conjugation and natural affinity to DNA make it possible to functionalize DNA structures with the heteroelements (proteins, small molecules, and nano- particles). A comprehensive list of the proteins functionalized on (or used for functionalization of) nanoscale DNA constructs is provided as a reference for the readers **(Table 1)**. DNA-assisted molecular and structural biophysics is concerned with understanding the structure, function and physicochemical properties of proteins and molecules using DNA as a tool/platform. The key to carry out such studies is positioning proteins and molecules on DNA nanostructures at spatially addressable locations with high precision.

3.1.1 High-precision positioning of molecules

Single molecules studies often require isolated molecules in an environment suitable for measurements. Nanoscale precision offered by DNA-based construction has been used to place molecules at specific locations on 2D platforms and arrays in several studies. Recently, a two-armed DNA origami hinge device has been used to control the positioning of molecules with very high precision (Figure 9(A)) [112]. The angle between the two arms of the hinged device can be controlled by adjuster helices placed between the arms, with increasing lengths of the adjuster helices resulting in higher angles between the arms (thus larger distances between molecules attached on each of the arms). This system was used to study distance-dependent dye interactions and fluctuation- dependent crosslinking interactions between bismaleimide and thiol groups. The positioning capabilities of the device were tested with photophysical and crosslinking assays, which report the co-ordinates of interest with very high resolution, reaching atomic length scale. Measurements revealed that the smallest displacement step possible was 0.4 Å, which is slightly lesser than the Bohr radius (0.529 Å). This study reinforces the possibility of placing molecules on DNA nanostructures at very high resolution, a key to do high-resolution single molecule structural studies—thereby bolstering the concept of molecular scaffolding.

3.1.2 Exploring the unwrapping of nucleosomes using DNA-origami

DNA origami hinge devices like the one described above have been used to study nucleosomes—the fundamental unit of eukaryotic chromosomes, a complex of DNA and histone proteins [113]. The hinged DNA origami device was used to analyze the unwrapping of nucleosomes as a function of ionic strength [114]. The nucleosome particle was attached via single stranded DNA handles to the two arms of the hinged device (Figure 9(B)). As the ionic strength increased (concentration of NaCl), unwrapping of the nucleosomes caused the release of the nucleosome particle from the origami device—this resulted in the observation of a larger angle between the arms of the device. This device has also been used to study distance-dependent interactions between two nucleosome particles by attaching one nucleosome on each arm of the hinged device (Figure 9(C)) [115]. The distance dependent interaction energy landscape between nucleosomes was discerned using electron microscopy image analysis and FRET measurements. In another study, similar DNA nanocalipers were used to investigate the wrapping of nucleosomes by DNA linkers of different lengths (Figure 9(D)) [116].

3.1.3 Single-molecule force spectrometers

Single molecule spectroscopy is a highly promising technique to understand the folding pathways and elastic response of macromolecules [117–119]. Two main drawbacks to this technique still persist: limited data throughput and noise incurred by the use of connector molecules report the events at a macroscopic scale. The former limitation can be addressed by parallel data acquisition from multiple events while the latter can be aided by the use of nanoscopic connectors that can sense minute conformational changes with minimal noise. To address this issue, rigid DNA origami beams have been used for single molecule force spectroscopy experiments [120–122]. This concept has been used to build a nanoscopic force clamp that allows autonomous operation and massively parallels data collection [121]. The device consisted of a bracket-shaped DNA origami clamp with a single stranded DNA spring extending within the space of the clamp (Figure 9(E)). Single- stranded DNA molecules of different lengths attached to the molecule of interest act as entropic springs, with shorter strands exerting more force. This design was used to study the conformational transitions of a Holliday junction (Figure 9(F)) as well as DNA bending induced by TATA-binding protein. In another report, Dietz and co-workers studied the stacking forces in DNA using a DNA origami-based single-molecule device coupled with dual beam optical trap [122].

3.2 DNA nanostructures for structure elucidation of macromolecules

3.2.1 Aligning proteins with DNA origami nanotubes for NMR studies

Nuclear magnetic resonance (NMR) measurements can be used to determine the structures of small membrane proteins (up to 40kDa). Controlled reintroduction of anisotropic residual dipolar coupling (RDC) provides high- resolution structural features of the macromolecules under study. Partial directional averaging of proteins in liquid crystalline media enables the measurement of RDCs. In addition to retaining conditions for solution-state high resolution NMR, a detergent-resistant weak alignment media is preferred for aligning

membrane proteins. DNA origami based liquid crystalline media, which is detergent-resistant and functioning at a range of pH, is suitable to achieve transient weak alignment of membrane proteins. Six-helix DNA origami bundles (a heterodimer of two long bundles) have been used to provide such a weak alignment medium for protein structure determination (Figure 10(A), top) [123]. This long DNA origami tube was used to align and collect anisotropic RDCs of a 40kDa tetrameric BM2 channel protein reconstituted in detergent micelles and aided in solving the structure de novo [123, 124]. These DNA nanotubes have also been used to determine the high resolution (backbone) structure of mitochondrial uncoupling protein 2 (UCP2), a membrane protein that facilitates the transport of small molecules across the mitochondrial inner membrane (Figure 10(A), bottom) [125].

3.2.2 Cryo-EM structure determination of proteins using DNA-based molecular supports

Holliday junctions tailed with sticky ends have been used to construct 2D arrays and to host junction-binding proteins such as RuvA [126]. Specifically designed four-arm junctions assemble into a trigonal 2D crystalline array (Figure 10(B), top). These lattices were used to arrange a 40 kDa guanine nucleotide binding protein Gαi1, rat neurotensin receptor type 1 (NTS1, a 43 kDa protein), and the signaling complexes of NTS1 with Gαi1 in a 2D array [127]. Attachment of proteins on the DNA array was facilitated by N-terminal His-tags on the protein and a tris-nitrilotriacetic acid (tris-NTA) modification on one of the component DNA strands of the junction unit. These arrays were analyzed by cryo-electron microscopy (Cryo-EM), which usually requires a large number of particle images for high- resolution 3D reconstruction (Figure 10(B), bottom). Such 2D DNA nanoaffinity templates can be used to create dense non-overlapping arrays of protein molecules for structure determination of aperiodic single-particles using Cryo-EM, while also allowing high-throughput data collection.

Structural elucidation of computer-designed DNA origami structures would aid in better designing of artificial nanomachines and highly rigid structures (at high resolutions), which in turn could act as molecular scaffolds to image small proteins and molecules that are attached to them. Since the advent of new detectors and aberration-corrected electron microscopes, single-particle cryo-EM is becoming an increasingly important tool to elucidate the structures of uncrystallized aperiodic single-macromolecules [128–130]. At the time of this review preparation, there has been only one reconstructed structure of 3D DNA origami available at a reasonable resolution, that of a compact hand-shaped 3D DNA origami structure using cryo-EM, with an overall resolution of 11.5 Å, with the resolution ranging from 9.7 Å at the core to 14 Å at the periphery (Figure 10(C)) [131]. This densely packed structure possessed a few unique unnatural DNA topologies such as vertical stack of five Holiday junctions and left-handed pseudohelices. The study of DNA origami structures using cryo-EM led to the use of such constructs as molecular supports for structure elucidation of other biomolecules. For example, a hollow DNA origami cage has been used as a molecular support to study the transcription factor p53 using cryo-EM [132]. The cavity of the DNA origami cage contains a single double helix with a specific sequence that the protein can bind to (Figure 10(D)). Moreover, by controlling the position of this sequence, the orientation of the protein in this cage can also

likely be controlled and analyzed using cryo-EM. Such DNA cages also likely protect the confined proteins from external harsh environments in EM studies.

3.3 DNA nanostructures for plasmonic/photonic materials

Spatially addressable arrangement and assembly of atoms, molecules, and nanoparticles at the nanoscale or sub-nanoscale level are crucial steps to achieve the goals of nano- technology. Gold and silver nanoparticles (Au/Ag NPs) are the widely used nanoparticle systems in DNA-metal hybrid assembly. While there are reports on other semiconductor nanoparticle systems whose surfaces can be modified, the facile nature of functionalizing and attaching DNA on the surface of AuNPs, coupled with the nanoscale phenomenon of surface plasmon resonance in the visible range makes AuNPs the most utilized candidate in DNA-metal hybrid systems. The assembly of AuNPs into reversible macroscopic aggregates using thiol-modified oligonucleotides [133] and the precise positioning of small AuNPs on a dsDNA template [134] laid the foundation for DNA-based nanoparticle assembly. Since then, the community has made large strides in assembling a gamut of nanoparticle systems using DNA. Some examples include AuNPs arranged into 2D lattices using DNA origami nanoflowers [135], size-selective placement on a triangular origami structure [136], periodic AuNP lattices [35], and binary mixtures of anisotropic nanoparticles [137]. DNA-based positioning of nanoparticles at spatially addressable locations on complex nanoscale structures lead to emergent properties with applications as plasmonic materials [138].

With molecular self-assembly, control and arrangement of nanomaterials in complex geometries in three-dimensions can be achieved more easily at the nanoscale than with the conventional lithographic approaches. DNA, with its programmable nature, allows the assembly of plasmonic/photonic materials in desired geometries with nanoscale precision and high fidelity [139–141]. For example, DNA origami nanotubes have been used to create chiral AuNP assemblies that exhibited characteristic bisignate signatures in the visible range (Figure 11(A)) [142]. In another example, 2D DNA origami sheets functionalized with linear chains of gold nanoparticles were rolled into DNA tubes to create gold nanohelices exhibiting chiral characteristics (Figure 11(B)) [143]. Similarly, a 3D plasmonic chiral AuNP tetramer has also been assembled using a 2D origami rectangle (Figure 11(C)) [144]. A DNA origami-based reconfigurable plasmonic nanosystem that can be controlled by toehold-based strand displacement has also been developed [145]. In this case, the origami structure had two 14-helix bundles connected in the middle, each of which carries a gold nanorod (Figure 11(D)). By introducing specific DNA strands, the arms of the bundles can be connected to create a right- or left-handed optical response. DNA-functionalized gold nanorod plasmonic walkers have been designed to take nanoscale steps on a DNA origami platform [146]. The progressive steps made by the walker trigger a series of conformational changes to the plasmonically coupled system, thus giving rise to immediate spectral response changes. This dynamic walking process can be read out using optical spectroscopy (Figure 11(E)) [147]. Moreover, in this system, the optical response can be tailored by modifying the number of walkers. Such a system allows monitoring of nanoscale loco- motion on the order of several nanometers, which is far below the optical resolution limit.

Precise assembly of nanoparticles into crystalline and open 3D frameworks has also been achieved by connecting them through designed DNA-based polyhedral frames [148, 149]. DNA-based binding of nanoparticles to these frames, along with the geometry of the designed frames allows defined connections and architectures (Figure 11(F)). Such DNA origami frames can be used to fabricate metal clusters with various symmetries and particle compositions, and to create nanoclusters with different chiroptical activities [150]. For example, toroidal metamolecules have been created using circular DNA origami frames and AuNPs (Figure 11(G)) [151]. In addition to spherical nanoparticles, gold nanorods (AuNRs) assembled on 2D DNA origami templates have been shown to exhibit strong chiroptical activities [152]. Bifacial DNA origami has been used as a template to create discrete anisotropic AuNR dimer nanoarchitectures (Figure 11(H)) [153]. In this system, the 3D spatial configuration was precisely tuned by rationally shifting the location of AuNRs on the origami template. This strategy was further extended to create AuNR helical superstructures with tailored chirality by designing a cross-shaped arrangement of DNA capturing strands on both sides of the 2D DNA origami template (Figure 11(I)) [154]. AuNRs functionalized with complementary DNA strands bind to the origami template and assemble into AuNR helices with the origami intercalated between adjacent AuNRs. Such precise arrangement of metal particles on DNA origami has also been shown to be a viable tool for the creation surface-enhanced Raman scattering (SERS)-active nanoparticle assemblies (Figure 11(J)) [155]. In a recent report, an AuNP was designed to perform a stepwise 'roll' directionally and progressively on DNA origami, while another AuNP was used as a stator [156]. The inter-particle distance variation generated by the rolling of the AuNP reporter was monitored by SERS. This method could be used as an optical reporter to monitor inter-particle variations in plasmonic nanostructures. Self-similar (similar to part of itself) chains of metal nanoparticles can create nanolenses, which provide extremely high field enhancements. Heck et al created gold nanolenses by connecting gold nanoparticles, which are similar, but different in size, using DNA origami [157]. They placed 10, 20, and 60 nm spherical gold nano- particles extremely close to each other in different geometrical arrangements on a triangular DNA origami shape using sticky ends. They studied the field enhancement effect by placing dye molecules on nanoparticles and measuring SERS as a function of geometrical arrangement of three particles and inter-particle distances. The 20-10-60 nm particle arrangement on DNA origami resulted in the maximum field enhancement matching theoretical expectations of a cascaded field enhancement effect. Zhan et al demonstrated a controlled shift of the plasmonic resonance peak by aligning gold nanorods on a DNA origami tripod [158]. The angle between the legs was controlled by toehold-based strand displacement, in turn resulting in reconfigurable plasmonic properties. The distinct electromagnetic response from the tripod shapes matched the calculated response as a function of angle between the legs. At this point, we point the reader to a recent review article by Liu and colleagues that discusses DNA nanotechnology-based chiral plasmonic architectures in great detail [159].

3.4 DNA nanostructures in fluorescence imaging

Apart from the assembly of plasmonic materials discussed above, DNA-based constructs have been used in assembling fluorescent materials/molecules (for examples, quantum dots or fluorophores) [160–162] and in

fluorescence imaging. The ability to functionalize DNA-based structures with fluorophores at spatially addressable locations with high precision makes it useful as fluorescence nanoscale rulers [163], sensors [164], and molecular switches for probing the dynamics of sub-cellular structures and events [165, 166]. Such structures are also used to engineer the photo-physical properties of QDs/fluorophores and to create smart photonic and light harvesting devices [161, 167–170]. For instance, fluorophores strategically placed in the plasmonic hot spot using DNA would exhibit several fold enhanced fluorescence [171].

Lin et al created a fluorescent barcode using a rigid DNA origami rod with multiple fluorescent tags (Figure 12(A)) [172]. Previously, fluorescence barcoding work with DNA tile arrays had been carried out for the biosensing of nucleic acids [164]. More recently, DNA origami based meta- fluorophores have been introduced, where fluorophores are densely packed on a DNA origami platform (132 dyes on a 60 × 30 nm2 origami) [173]. The brightness and color of the metafluorophores can be tuned to create a pallet of 124 virtual colors. These metafluorophores were used as high throughput nucleic acid detection sensor (Figure 12(B)).

Stochastic super-resolved fluorescence imaging techniques [174, 175] take advantage of the 'on' and 'off' states of fluorophores. The base pair recognition and hybridization principle of DNA coupled with the Points Accumulation for Imaging in Nanoscale Topography (PAINT) [176] led to a versatile imaging method DNA-PAINT [177]. This method achieves the stochastic blinking of fluorophores through transient binding of free-floating imager DNA-strand (labeled with fluorophore) that docks with the target complementary strand (Figure 12(C)). Fluorescence is detected only in bound states (on) and once the strand dissociates it does not fluoresce anymore (off). This allows imaging cellular structures at molecular or super resolution even with normal epi-fluorescence or confocal microscopes. This method not only enables super-resolved optical imaging of sub-cellular structures but also aids the optical characterization of DNA-based nanostructures and assemblies. For example, polyhedra assembled from DNA origami tripods have been characterized in solution using the DNA-PAINT method (Figure 12(D)) [60]. Previously, Shih and co-workers studied the motor movements of dyenin and kinesin on DNA origami tubes and used DNA-PAINT to characterize the spacing (~28 nm) between the adjacent protein molecules on the protein–DNA origami construct [178]. Further, newer versions of this method such as quantitative-PAINT and exchange-PAINT have been demonstrated using DNA origami structures [179–182]. Nollman and his colleagues applied DNA-PAINT method to collect thousands of 2D fluorescence images of a DNA origami tetrahedron in solution in a microfluidic chamber [183]. They classified the images into class averages and reconstructed the 3D structure by applying angular reconstitution in combination with multivariate statistics method (following the methods developed for 3D cryo-EM imaging—but the signal here is emitted photons from the fluorophores) (Figure 12(E)). The computationally designed, well characterized DNA origami objects labeled with fluorophores act as excellent model samples for the imaging method development [183].

Steinhauer et al demonstrated the concept of DNA-based nanoscale ruler for super-resolution fluorescence microscopy with a rectangular 2D DNA origami labeled with two fluorophores separated by a distance below the diffraction limit [163]. Since then, DNA origami objects labeled with fluorophores with inter-fluorophore distances below the diffraction limit have become standard nanoscopy rulers in super-

resolution microscopy. Schmied et al further developed this concept with various 3D DNA origami shapes, and showed that fluorophores could be placed within ~5 nm next to each other and still be resolved (Figure 12(F)) [184–186]. Recently, Hell and his col- leagues used DNA origami objects as test samples and nanoscale fluorescence rulers to demonstrate a new variant of super- resolution imaging method MINFLUX (MINimal emission FLUXes), achieving nanometer resolution while utilizing fewer number of emitted photons than before [187]. Readers may refer to the recent review by Jungmann and co-workers for further information on the applications of DNA nanotechnology in fluorescence imaging [188].

4. Summary and perspective

With the expanding tools of structural biology, what DNA nanotechnology has to offer to the biophysical community is an important question. DNA nanostructures have been used as custom-designed model systems for method development of imaging techniques, as molecular scaffolds to obtain molecular structure of guests, to assemble or align molecules, as molecular beacons/sensors/spectrometers to probe a chemical or physical process, and as nanoscale rulers. 3D assembly of plasmonic materials in complex geometries has now become routine with DNA-based assembly routes; such constructs would be useful in probing intracellular events with dark field microscopy coupled with spectroscopy [189, 190]. DNA origami nanorulers have become standards in fluorescence microscopy and the technology has already been commercialized. As we noted above, DNA origami tubes have been used to align membrane proteins for high-resolution NMR structure determination. Cryo-EM has undergone rapid developments in the past few years in terms of resolution and the size of the macromolecules that can be imaged [191–194]. While it has become possible to determine the 3D structures of sub-100 kDa protein molecules directly with cryo-EM [194, 195], DNA based molecular supports still offer the possibility of imaging much smaller proteins/macromolecules attached to such sup- ports as well as to study the forces or interaction energy landscape between macromolecules using unique unnatural constructs [115, 127, 132].

Highly intense femtosecond pulses of x-ray free electron lasers (XFEL) offer the possibility of imaging the structure and dynamics of biomolecules and macromolecular complexes frozen in time at room temperature while outrunning radiation damage [196–202]. XFEL single-particle diffractive imaging is in its early stages of development [203–205]. A key challenge in this emerging lensless imaging technique is measuring the weak diffraction signal of a single biomolecule above the background noise at high-resolution in a single-shot with an x-ray laser pulse. DNA nanotechnology has a lot to offer to XFEL imaging techniques and would likely be useful to orient single macromolecules arbitrarily without the need to strictly position the molecules in the crystallographic lattice positions. Such an alignment strategy would yield enhanced signal while minimizing the orientation determination problem, and can be used to reconstruct the 3D structure of weakly scattering single biomolecules at high resolution at room temperature without the need for crystallization [206–208]. For instance, single-molecules could be rigidly attached to DNA origami tubes and flow-aligned in a low- background, ultra-thin liquid-jet to obtain single-shot, single molecule diffraction with XFEL pulses, where the DNA nanostructure could also act as a holographic reference to the

target molecule [209]. Furthermore, custom-designed DNA origami objects/molecular scaffolds would be excellent model samples for XFEL imaging method development [203].

On the other hand, the expanding gamut of biophysical tools offers the possibility to characterize and understand DNA-based nanostructures and assemblies in unprecedented detail. Innovations in nanoscopic tools would enable the observation of assembly process and structural dynamics of DNA nanostructures at higher resolution and faster timescales than currently possible at the single molecule level [210]. For instance, high-speed atomic force microscopy (AFM) has been used to image light-induced dynamics in DNA nanostructures and the possibilities to visualize a range of dynamics with different triggers (temperature, pH) and the dynamics of protein–DNA nanostructure interactions are quite evident [211, 212]. Other emerging techniques such as liquid phase single-particle imaging with electrons [213–215] may help understand the assembly of higher order DNA objects in solution at electron microscopy resolution; such studies are now carried out with AFM [216]. In addition, upcoming nanoscale imaging techniques such as low-energy electron diffraction [217], 3D super-resolved fluorescence imaging [183, 218], static and time resolved cryo-EM [219, 220], coherent diffractive single-particle imaging [205, 221, 222] and incoherent diffractive imaging (quantum imaging) with XFEL utilizing the fluorescence from the phosphorous (P) in nucleic acids [223, 224] would enable unique experiments with DNA-based architectures and bring new understanding of DNA nanostructures and machines. Empirical mapping of the conformational energy landscape of DNA nanostructures has concomitantly become feasible through single-molecule structural studies. Ultrafast imaging techniques [204, 210, 223–227] which utilize ultra-short (femto- and attosecond (fs/as)) pulses would likely enable us to understand the charge transfer and other ultra-fast processes in DNA nanostructures and DNA-based photonic/plasmonic constructs at the elementary (fs/as) timescales of atomic and electronic motions.

Conventional spectroscopic, crystallographic, and scattering techniques investigating ensembles would still be beneficial and relevant to investigate DNA nanostructures. Small angle x-ray scattering (SAXS) has been used to analyze an ensemble of DNA nanostructures in solution [228]. For example, synchrotron or home-source based SAXS has been used to analyze interhelical spacing in sheet-, brick-, and cylinder-shaped DNA origami constructs as a function of temperature and Mg2+ ion concentration [228] and to study conformational changes and flexibility in DNA devices [229]. Time-resolved fluorescence studies have also been carried out to study energy transfer between strategically positioned dyes (akin to a photonic wire) on a DNA origami platform [230]. The original goal of designing 3D DNA crystals to accommodate guest molecules is still relevant and new techniques like room temperature serial femtosecond crystallography (SFX), which simultaneously opens up ultrafast time resolved studies [197, 231] and cryogenic micro-electron diffraction (micro-ED) [232] have relaxed the size limits of crystals. With such advanced techniques, certain crystal imperfections might even lead to better resolution reconstruction [206]. Crystals with specific translational disorder produce continuous diffraction—the incoherent sum of the elastic scattering signal of each three dimensionally aligned single molecule—apart from Bragg spots (the coherent sum). In a recent SFX experiment, using only continuous diffraction signal, the single-molecule structure was reconstructed by applying coherent diffractive imaging technique's iterative phasing leading to

a resolution beyond Bragg spots [206]. Certain flexibility and disorder of DNA crystalline scaffolds could be tolerated and might in fact be beneficial in the SFX method [199, 233]. Perhaps, engineering the translational symmetry of molecules to produce only continuous diffraction and getting rid of Bragg spots in a suitably sized DNA nanocrystal/scaffold (single to a few unit cells) might open up a new avenue of DNA-assisted single particle imaging with XFEL, since multiple copies of the molecules in the same orientation with tolerable translational disorder would provide amplified single-molecule signal [233]. Attempts to crystallize DNA origami structures (~4.8 MDa) have been made and a DNA origami tensegrity triangle was recently assembled into a 3D array [74], but solving the crystal structure of such origami lattices has been challenging due to the inherent flexibility and heterogeneity of the cohering units [47]. Highly rigid, non-heterogeneous and defect-free 3D DNA nanoscale origami shapes at high-resolution (atomic/ near-atomic) need to be realized yet. Given the pace at which the field is progressing, with the advancements in computational tools for design and stability analysis, and synthesis methods, this seems feasible. Here, one needs to note that the increasing understanding of biological machines at high resolutions indicates that (conformational) heterogeneity in biology is quite common—and it is not completely an undesirable quality in artificial machines, although perfection is preferred.

Assembly of nanostructures based on DNA has been thoroughly studied in recent times for the kinetic and thermodynamic constraints [234]. For DNA origami, various strategies have been used to construct a variety of shapes, and in addition, the folding pathways of origami have been optimized for better yields [235, 236]. Advances in design of such structures also allow more control over their growth and assembly [237]. The size of DNA origami nanostructures is limited by the length of the scaffold strand, with a majority of DNA origami structures today constructed using the ~7 kb M13 single stranded scaffold [52]. This limitation is now addressed by creating scaffolds ranging in length from ~700 to ~50 000 nucleotides using different strategies (Figure 13) [60, 238–242]. Thus one can choose from a library of scaffold strands to build nanostructures of desired sizes (Figure 12) [243]. Earlier construction of DNA nanostructures involved a thermal annealing process. While many assemblies still have this as a requirement, recent successes in isothermal assembly has made the creation of DNA nanostructures feasible for protein–DNA hybrids since proteins or peptides do not survive the high temperatures during the annealing process [244–249]. Enzymatic production of DNA strands is another feature that aids the large scale production of DNA-based nanostructures [250], as well as using a limited set of reusable sequences to fold a desired origami structure [251]. Moreover, the cost of producing such DNA structures can be reduced by using chip-synthesized oligonucleotides [252–254]. In addition, intact bacteriophages have been used to assemble DNA origami structures [255], and very recently, biotechnological mass production of DNA origami has also been demonstrated—heralding the beginning of industrial scale DNA nanotechnology [256]. One other requirement for most DNA nanostructures is their purification after assembly [257]. Many different purification strategies have been developed for this purpose, including rate-zonal centrifugation [258, 259], PEG-based separation [123, 259, 260], size exclusion columns [259, 261], spin filters [262], magnetic bead capture [259], liquid chromatography-based techniques [263] free-flow electrophoresis [264] and the routinely used method based on agarose gel electrophoresis extraction [259, 265].

The versatility of DNA based construction has resulted in a wide variety of heterogeneous complexes. Aided by advances in chemical synthesis of DNA strands with desired functional groups, almost any guest can be attached to an underlying motif or an origami structure. Click-based functionalization [266, 267] and recognition of DNA by functional ligands and triplexes [268, 269], for example, are other routes to functionalizing designer DNA architectures. Moreover, recent efforts have demonstrated the use of xeno nucleic acids [270] in DNA nanostructures, and could be expanded to include modified nucleotides [271] and non-traditional base pairs [272]. Moreover, incorporation of unnatural base pairs has been shown to enhance the stability of DNA nanostructures [273] and can thus lead to construction of more robust architectures. It is worth noting that RNA nanostructures and RNA-based origami are also emerging following the footsteps of DNA nanotechnology [274, 275]. Simplicity in designing nanostructures and positioning molecules at spatially addressable locations in the case of nucleic acid nanostructures is the key advantage over other biomolecular constructs. With increasing understanding of the design rules [8], designer protein materials have also started to play significant roles in the development of bionanomaterials and biophysical applications [276, 277]. We envisage a high degree of synergy between protein-based designer materials and artificial nucleic acid nanostructures in the future leading to much sophisticated mimics of bio-machineries with novel functions.

Other areas of applications we did not cover in this review include drug delivery and biosensing. DNA nano-carriers show enhanced stability in biological environments [278, 279] and have been used to encapsulate cargos such as doxorubicin [280], CpG motifs [281], siRNA [282], proteins [283] and metal complexes [284]. In the biosensing aspect, DNA based biosensors have been used to detect both protein [285] and nucleic acid targets [286]. The amalgamation of DNA nanotechnology with lithography has unique potential in the area of sensors and molecular electronics [287–290]. Dynamic DNA devices and self-replicating nanomachines are also another active area of research [291–294]. DNA nanostructures on membranes have applications in the synthetic biology and will likely help in building synthetic bio- systems [295]. A systems biology approach and multiscale modeling of hierarchical assemblies of DNA nanostructures and their interaction with proteins would improve the understanding of emergent behavior in higher ordered structures. Such studies would likely shed light on chromosomal (~TDa scale) organization, structure and dynamics. Besides, DNA has been used in computational platforms and memory devices for information storage and processing [296–303]. These applications converge as sensing can be coupled with drug carriers, so they can be triggered open to release the cargo on environ- mental cues. With specific information stored in such DNA carriers, the response to a specific biomarker can be read out in a variety of signal outputs. With all these intriguing properties, and the emergent applications, DNA is probably the 'twist' on the voyage of science fiction becoming a reality.

Acknowledgements

PLX thanks advisors H N Chapman and N C Seeman for inducting into DNA nanotechnology and for stimulating discussions and acknowledges the support of the International Max-Planck Research School for Ultrafast Imaging and Structural Dynamics (IMPRS-UFAST) of the Max-Planck Society, graduate student training program of the Linac Coherent Light Source (LCLS, Stanford), the European Research Council—Frontiers in Attosecond X-ray Science: Imaging and Spectroscopy (AXSIS), the Human Frontiers Science Program, and the Helmholtz Association.

ORCID iDs

P Lourdu Xavier 0000-0001-5132-2999
Arun Richard Chandrasekaran 0000-0001-6757-5464

References

1. Seeman NC (2016) Structural DNA Nanotechnology, Cambridge University Press.

2. Jones MR, Seeman NC and Mirkin CA (2015) Programmable materials and the nature of the DNA bond. Science 347, 1260901.

3. Seeman NC (2003) DNA in a material world. Nature 421, 427-431.

4. Feynman RP (1960) There's plenty of room at the bottom. Engineering and Science, 23, 22-36.

5. Heinrich AJ, Lutz CP, Gupta JA and Eigler DM (2002) Molecule Cascades. Science 298, 1381-1387.

6. Eigler DM and Schweizer EK (1990) Positioning single atoms with a scanning tunnelling microscope. Nature 344, 524-526.

7. Seeman NC, Belcher AM (2002) Emulating biology: building nanostructures from the bottom up. Proc. Natl. Acad. Sci. U. S. A. 99, 6451-6455.

8. Huang PS, Boyken SE and Baker D (2016) The coming of age of de novo protein design Nature 537, 320-327.

9. Bale JB, Gonen S, Liu Y, Sheffler W, Ellis D, Thomas C, Cascio D, Yeates TO, Gonen T, King NP and Baker D (2016) Accurate design of megadalton-scale two-component icosahedral protein complexes. Science 353, 389-394.

10. Yatsunyk LA, Mendoza O and Mergny JL (2014) "Nano-oddities": unusual nucleic acid assemblies for DNA-based nanostructures and nanodevices. Acc. Chem. Res. 47, 1836-1844.

11. Meng HM, Liu H, Kuai H, Peng R, Mo L, Zhang XB (2016) Aptamer-integrated DNA nanostructures for biosensing, bioimaging and cancer therapy. Chem. Soc. Rev. 45, 2583-2602.

12. Wang F, Lu CH and Willner I (2014) From cascaded catalytic nucleic acids to enzyme-DNA nanostructures: controlling reactivity, sensing, logic operations, and assembly of complex structures. Chem Rev. 114, 2881-2941.

13. Seeman NC (1982) Nucleic-acid junctions and lattices. J. Theor. Biol. 99, 237-247.

14. Holliday R (1964) A mechanism for gene conversion in fungi. Genet. Res. 5, 282-304.

15. Kallenbach NR, Ma RI and Seeman NC (1983) An Immobile nucleic acid junction constructed from oligonucleotides. Nature 305, 829-831.

16. Wang Y, Mueller JE, Kemper B and Seeman NC (1991) The assembly and characterization of 5-arm and 6-arm DNA junctions. Biochemistry 30, 5667-5674.

17. Wang X and Seeman NC (2007) The assembly and characterization of 8-arm and 12-arm DNA branched junctions. J. Am. Chem. Soc. 129, 8169-8176.

18. Chen J and Seeman NC (1991) The synthesis from DNA of a molecule with the connectivity of a cube. Nature 350, 631-633.

19. Zhang Y and Seeman NC (1994) The construction of a DNA truncated octahedron, J. Am. Chem. Soc. 116, 1661-1669.

20. Shih WM, Quispe JD and Joyce GF (2004) A 1.7-kilobase single-stranded DNA that folds into a nanoscale octahedron. Nature 427, 618-621.

21. Bhatia D, Mehtab S, Krishnan R, Indi SS, Basu A and Krishnan Y (2009) Icosahedral DNA nanocapsules by modular assembly. Angew. Chem. Int. Ed. 48, 4134-4137.

22. Goodman RP, Schaap IA, Tardin CF, Erben CM, Berry RM, Schmidt CF, Turberfield AJ (2005) Rapid chiral assembly of rigid DNA building blocks for molecular nanofabrication. Science 310, 1661-1665.

23. He Y, Ye T, Su M, Zhang C, Ribbe AE, Jiang W and Mao C (2008) Hierarchical self-assembly of DNA into symmetric supramolecular polyhedra. Nature 452, 198-201.

24. Zhang C, Ko SH, Su M, Leng Y, Ribbe AE, Jiang W and Mao C (2009) Symmetry controls the face geometry of DNA polyhedra. J. Am. Chem. Soc. 131, 1413-1415.

25. Zhang C, Su M, He Y, Zhao X, Fang P, Ribbe AE, Jiang W and Mao C (2008) Conformational flexibility facilitates self-assembly of complex DNA nanostructures. Proc. Natl. Acad. Sci. U. S. A. 105, 10665-10669.

26. Aldaye FA and Sleiman HF (2007) Modular access to structurally switchable 3D discrete DNA assemblies. J. Am. Chem. Soc. 129, 13376-13377.

27. Chandrasekaran AR and Levchenko O (2016) DNA Nanocages. Chem. Mater. 28, 5569-5581.

28. Seeman NC (1985) Macromolecular design, nucleic acid junctions and crystal formation. J. Biomol. Struct. Dyn. 3, 11-34.

29. Fu TJ and Seeman NC (1993) DNA double-crossover molecules. Biochemistry 32, 3211-3220.

30. LaBean T, Yan H, Kopatsch J, Liu F, Winfree E, Reif JH and Seeman NC (2000) The construction of DNA triple crossover molecules. J. Am. Chem. Soc. 122, 1848-1860.

31. Shen Z, Yan H, Wang T, Seeman NC (2004) Paranemic crossover DNA: a generalized Holliday structure with applications in nanotechnology. J. Am. Chem. Soc. 126, 1666-1674.

32. Ohayon YP, Sha R, Flint O, Chandrasekaran AR, Abdallah HO, Wang T, Wang X, Zhang X, Seeman NC (2015) Topological linkage of DNA tiles bonded by paranemic cohesion. ACS Nano 9, 10296-10303.

33. Ohayon YP, Sha R, Flint O, Liu W, Chakraborty B, Subramanian HK, Zheng J, Chandrasekaran AR, Abdallah HO, Wang X, Zhang X, Seeman NC (2015) Covalent linkage of one-dimensional DNA arrays bonded by paranemic cohesion. ACS Nano 9, 10304-10312.

34. Seeman NC, Wang H, Yang X, Liu F, Mao C, Sun W, Wenzler L, Shen Z, Sha R, Yan H, Wong MH, Sa-Ardyen P, Liu B, Qiu H, Li X, Qi J, Du SM, Zhang Y, Mueller JE, Fu TJ, Wang Y and Chen J (1998) New motifs in DNA nanotechnology. Nanotechnology 9, 257.

35. Sharma J, Chhabra R, Liu Y, Ke Y, Yan H (2006) DNA-templated self-assembly of two-dimensional and periodical gold nanoparticle arrays. Angew. Chem. Int. Ed. 45, 730-735.

36. Park SH, Yin P, Liu Y, Reif JH, LaBean TH and Yan H (2005) Programmable DNA self-assemblies for nanoscale organization of ligands and proteins. Nano Lett. 5, 729-733.

37. Chandrasekaran AR and Zhuo R (2016) A 'tile'tale: Hierarchical self-assembly of DNA lattices. Appl. Mater. Today 2, 7-16.

38. Chandrasekaran AR (2016) Programmable DNA scaffolds for spatially-ordered protein assembly. Nanoscale 8, 4436-46.

39. Zheng J, Birktoft JJ, Chen Y, Wang T, Sha R, Constantinou PE, Ginell SL, Mao C and Seeman NC (2009) From molecular to macroscopic via the rational design of a self-assembled 3D DNA crystal. Nature 461, 74-77.

40. Liu D, Wang M, Deng Z, Walulu R and Mao C (2004) Tensegrity: Construction of rigid DNA triangles with flexible four-arm dna junctions. J. Am. Chem. Soc. 126, 2324-2325.

41. Nguyen N, Birktoft JJ, Sha R, Wang T, Zheng J, Constantinou PE, Ginell SL, Chen Y, Mao C and Seeman NC (2012) The absence of tertiary interactions in a self-assembled DNA crystal structure. J. Mol. Recognit. 25, 234-237.

42. Wang T, Sha R, Birktoft J, Zheng J, Mao C and Seeman NC (2010) A DNA crystal designed to contain two molecules per asymmetric unit. J. Am. Chem. Soc. 132, 15471-15473.

43. Sha R, Birktoft JJ, Nguyen N, Chandrasekaran AR, Zheng J, Zhao X, Mao C, Seeman NC (2013) Self-assembled DNA crystals: the impact on resolution of 5'-phosphates and the DNA source. Nano Letters 13, 793-797.

44. Ohayon YP, Chandrasekaran AR, Hernandez C, Birktoft JJ, Sha R, Ginell S, Lukeman P, Mao C, Chaikin PM and Seeman NC (2015) Programmable crystal contacts used to improve the resolution of self-assembled 3D DNA crystals. J. Biomol. Struct. Dyn. 33, Suppl 1, 50-51.

45. Zhao J, Chandrasekaran AR, Li Q, Li X, Sha R, Seeman NC and Mao C (2015) Post-assembly stabilization of rationally designed DNA crystals. Angew. Chem. Int. Ed. 54, 9936-9939.

46. Abdallah HO, Ohayon YP, Chandrasekaran AR, Sha R, Fox KR, Brown T, Rusling DA, Mao C and Seeman NC (2016) Stabilisation of self-assembled DNA crystals by triplex-directed photo-cross-linking. Chem. Commun. 52, 8014-8017.

47. Stahl E, Praetorius F, de Oliveira Mann CC, Hopfner KP and Dietz H (2016) Impact of heterogeneity and lattice bond strength on DNA triangle crystal growth. ACS Nano 10, 9156-9164.

48. Rusling DA, Chandrasekaran AR, Ohayon YP, Brown T, Fox KR, Sha R, Mao C and Seeman NC (2014) Functionalizing designer DNA crystals with a triple-helical veneer. Angew. Chem. Int. Ed. 53, 3979-3982.

49. Wang X, Sha R, Kristiansen M, Hernandez C, Hao Y, Mao C, Canary JW and Seeman NC (2017) An organic semiconductor organized into 3D DNA arrays by "bottom-up" rational design. Angew. Chem. Int. Ed. 56, 6445-6448.

50. Hao Y, Kristiansen M, Sha R, Birktoft JJ, Hernandez C, Mao C and Seeman NC (2017) A device that operates within a self-assembled 3D DNA crystal. Nat Chem. 9, 824-827.

51. Hernandez C, Birktoft JJ, Ohayon YP, Chandrasekaran AR, Abdallah H, Sha R, Stojanoff V, Mao C, Seeman NC (2017) Self-assembly of 3D DNA crystals containing a torsionally stressed component. Cell Chem. Biol. DOI: 10.1016/j.chembiol.2017.08.018.

52. Rothemund PW (2006) Folding DNA to create nanoscale shapes and patterns. Nature 440, 297-302.

53. Douglas SM, Dietz H, Liedl T, Högberg B, Graf F and Shih WM (2009) Self-assembly of DNA into nanoscale three-dimensional shapes. Nature 459, 414-418.

54. Dietz H, Douglas SM and Shih WM (2009) Folding DNA into twisted and curved nanoscale shapes. Science 325, 725-730.

55. Andersen ES, et al (2009) Self-assembly of a nanoscale DNA box with a controllable lid. Nature 459, 73-76.

56. Han D, Pal S, Nangreave J, Deng Z, Liu Y and Yan H (2011) DNA origami with complex curvatures in three-dimensional space. Science 332, 342-346.

57. Zhang F, Jiang S, Wu S, Li Y, Mao C, Liu Y and Yan H (2015) Complex wireframe DNA origami nanostructures with multi-arm junction vertices. Nat. Nanotech. 10, 779-784.

58. Benson E, Mohammed A, Gardell J, Masich S, Czeizler E, Orponen P and Högberg B (2015) DNA rendering of polyhedral meshes at the nanoscale. Nature 523, 441-444.

59. Liu W, Zhong H, Wang R and Seeman NC (2011) Crystalline two-dimensional DNA-origami arrays. Angew. Chem. Int. Ed. Engl. 50, 264-267.

60. Iinuma R, Ke Y, Jungmann R, Schlichthaerle T, Woehrstein J B and Yin P (2014) Polyhedra self-assembled from DNA tripods and characterized with 3D DNA-PAINT. Science 344, 65-69.

61. Hong F, Zhang F, Liu Y, Yan H (2017) DNA Origami: Scaffolds for creating higher order structures. Chem Rev. DOI: 10.1021/acs.chemrev.6b00825

62. Wei B, Dai M and Yin P (2012) Complex shapes self-assembled from single-stranded DNA tiles. Nature 485, 623-626.

63. Ke Y, Ong LL, Shih WM and Yin P (2012) Three-dimensional structures self-assembled from DNA bricks. Science 338, 1177-1183.

64. Yin P, Hariadi RF, Sahu S, Choi HM, Park SH, Labean TH, Reif JH (2008) Programming DNA tube circumferences. Science 321, 824-826.

65. Zimmerman SC and Corbin PS (2000) Heteroaromatic Modules for Self-Assembly Using Multiple Hydrogen Bonds. In: Fuiita M. (eds) Molecular Self-Assembly Organic Versus Inorganic Approaches. Structure and Bonding, 96, 63-94.

66. Claessens CG and Stoddart JF (1997) π–π interactions in self-assembly J. Phys. Org. Chem. 10, 254-272.

67. Klosterman JK, Yamauchi Y and Fujita M (2009) Engineering discrete stacks of aromatic molecules. Chem. Soc. Rev. 38, 1714-1725.

68. Bowden N, Terfort A, Carbeck J and Whitesides GM (1997) Self-assembly of mesoscale objects into ordered two-dimensional arrays. Science 276, 233-235.

69. Zhao K and Mason TG (2007) Directing colloidal self-assembly through roughness-controlled depletion attractions. Phy. Rev. Lett. 99, 268301.

70. Nakata M, Zanchetta G, Chapman BD, Jones CD, Cross JO, Pindak R, Bellini T and Clark NA (2007) End-to-end stacking and liquid crystal condensation of 6– to 20–base pair DNA duplexes. Science 318, 1276-1279.

71. Wang R, Kuzuya A, Liu W and Seeman NC (2010) Blunt-ended DNA stacking interactions in a 3-helix motif. Chem. Commun. 46, 4905-4907.

72. Woo S and Rothemund PWK (2011) Programmable molecular recognition based on the geometry of DNA nanostructures. Nat. Chem. 3, 620-627.

73. Gerling T, Wagenbauer KF, Neuner AM and Dietz H (2015) Dynamic DNA devices and assemblies formed by shape-complementary, non–base pairing 3D components. Science 347, 1446-1452.

74. Zhang T, Hartl C, Fischer S, Frank K, Nickels P, Heuer-Jungemann A, Nickel B and Liedl T (2017) 3D DNA origami crystals. arXiv:1706.06965 [cond-mat.soft].

75. Aghebat Rafat A, Pirzer T, Scheible MB, Kostina A and Simmel FC (2014) Surface-assisted large-scale ordering of DNA origami tiles. Angew. Chem. Int. Ed. 53, 7665-7668.

76. Pastré D, Piétrement O, Fusil S, Landousy F, Jeusset J, David MO, Hamon L, Le Cam E and Zozime A (2003) Adsorption of DNA to mica mediated by divalent counterions: a theoretical and experimental study. Biophys J. 85, 2507-2518.

77. Suzuki Y, Endo M and Sugiyama H (2015) Lipid-bilayer-assisted two-dimensional self-assembly of DNA origami nanostructures. Nat. Commun. 6, 8052.

78. Mou Y, Yu JY, Wannier TM, Guo CL and Mayo SL (2015) Computational design of co-assembling protein-DNA nanowires. Nature 525, 230-233.

79. Praetorius F and Dietz H (2017) Self-assembly of genetically encoded DNA-protein hybrid nanoscale shapes. Science 355, eaam5488.

80. Elbaz J, Yin P and Voigt CA (2016) Genetic encoding of DNA nanostructures and their self-assembly in living bacteria. Nat. Commun. 7, 11179.

81. Seeman NC (1985) Interactive design and manipulation of macro-molecular architecture utilizing nucleic acid junctions. Journal of Molecular Graphics 3, 34-39.

82. Seeman NC (1990) De novo design of sequences for nucleic acid structural engineering. J. Biomol. Struct. Dyn. 8, 573-581.

83. Wei B, Wang Z, Mi Y (2007) Uniquimer: software of de novo DNA sequence generation for DNA self-assembly-an introduction and the related applications in DNA self-assembly. J. Comput. Theor. Nanosci. 4, 133-146.

84. Birac JJ, Sherman WB, Kopatsch J, Constantinou PE and Seeman NC (2006) Architecture with GIDEON, a program for design in structural DNA nanotechnology. J. Mol. Graph. Model. 25, 470-480.

85. Williams S, Lund K, Lin C, Wonka P, Lindsay S and Yan H (2008) Tiamat: a three-dimensional editing tool for complex DNA structures. In: Goel A, Simmel FC, Sosík P, (eds). The 14th International Meeting on DNA Computing Proceedings. Czech Republic: Silesian University in Opava, pages 112-121.

86. Zhu J, Wei B, Yuan Y and Mi Y (2009) UNIQUIMER 3D, a software system for structural DNA nanotechnology design, analysis and evaluation. Nucl. Acids Res. 37, 2164-2175.

87. Douglas SM, Marblestone AH, Teerapittayanon S, Vazquez A, Church GM and Shih WM (2009) Rapid prototyping of 3D DNA-origami shapes with caDNAno. Nucle. Acids Res. 37, 5001-5006.

88. Veneziano R, Ratanalert S, Zhang K, Zhang F, Yan H, Chiu W and Bathe M (2016) Designer nanoscale DNA assemblies programmed from the top down. Science 352, 1534.

89. Castro CE, Kilchherr F, Kim DN, Shiao EL, Wauer T, Wortmann P, Bathe M and Dietz H (2011) A primer to scaffolded DNA origami. Nat. Meth. 8, 221-229.

90. Maffeo C, Yoo J and Aksimentiev A (2016) De novo reconstruction of DNA origami structures through atomistic molecular dynamics simulation. Nucl. Acids Res. 44, 3013-3019.

91. Snodin BEK, Romano F, Rovigatti L, Ouldridge TE, Louis AA and Doye JPK (2016) Direct simulation of the self-assembly of a small DNA origami. ACS Nano 10, 1724-1737.

92. Kim DN, Kilchherr F, Dietz H, Bathe M (2012) Quantitative prediction of 3D solution shape and flexibility of nucleic acid nanostructures. Nucl. Acids Res. 40, 2862-2868.

93. Pan K, Kim DN, Zhang F, Adendorff MR, Yan H and Bathe M (2014) Lattice-free prediction of three-dimensional structure of programmed DNA assemblies. Nat. Commun. 5, 5578.

94. Pan K, Bricker WP, Ratanalert S and Bathe M (2017) Structure and conformational dynamics of scaffolded DNA origami nanoparticles. Nucl. Acids Res. 45, 6284-6298.

95. Chandrasekaran AR, Anderson N, Kizer M, Halvorsen K and Wang X (2016) Beyond the fold: Emerging biological applications of DNA origami. ChemBioChem 17, 1081-1089.

96. Linko V, Ora A and Kostiainen MA (2015) DNA nanostructures as smart drug-delivery vehicles and molecular devices. Trends Biotechnol. 33, 586-594.

97. Chen YJ, Groves B, Muscat RA and Seelig G (2015) DNA nanotechnology from the test tube to the cell. Nat. Nanotech. 10, 748-60.

98. Pei H, Zuo X, Zhu D, Huang Q and Fan C (2014) Functional DNA nanostructures for theranostic applications. Acc. Chem. Res. 47, 550-559.

99. Okholm AH and Kjems J (2017) The utility of DNA nanostructures for drug delivery in vivo. Expert Opin. Drug Deliv. 14, 137-139.

100. Chandrasekaran AR (2016) DNA origami and biotechnology applications: a perspective. J. Chem. Technol. Biotechnol. 91, 843-846.

101. Chandrasekaran AR (2016) Designer DNA architectures: Applications in nanomedicine. Nanobiomedicine 3, 6.

102. Angell C, Xie S, Zhang L and Chen Y (2016) DNA nanotechnology for precise control over drug delivery and gene therapy. Small 12, 1117-1132.

103. Chao J, Zhu D, Zhang Y, Wang L and Fan C (2016) DNA nanotechnology-enabled biosensors. Biosens. Bioelectron. 76, 68-79.

104. Krishnan Y and Bathe M (2012) Designer nucleic acids to probe and program the cell. Trends Cell Biol. 22, 624-633.

105. Chandrasekaran AR, Wady H and Subramanian HKK (2016) Nucleic acid nanostructures for chemical and biological sensing. Small 12, 2689-2700.

106. Chandrasekaran AR (2017) DNA nanobiosensors: an outlook on signal readout strategies. J. Nanomater. 2017, 2820619.

107. Lee JB, Campolongo MJ, Kahn JS, Roh YH, Hartman MR and Luo D. DNA-based nanostructures for molecular sensing. Nanoscale 2, 188-97.

108. Pei H, Zuo X, Pan D, Shi J, Huang Q and Fan C (2013) Scaffolded biosensors with designed DNA nanostructures. NPG Asia Materials 5, e51.

109. Teller C and Willner I (2010) Organizing protein-DNA hybrids as nanostructures with programmed functionalities. Trends Biotechnol. 28, 619-628.

110. Wilner O and Willner I (2012) Functionalized DNA Nanostructures. Chem. Rev. 112, 2528-2556.

111. Saccà B and Niemeyer CM (2011) Functionalization of DNA nanostructures with proteins. Chem. Soc. Rev. 40, 5910-5921.

112. Funke JJ and Dietz H (2016) Placing molecules with Bohr radius resolution using DNA origami. Nat. Nanotech. 11, 47-52.

113. Kornberg RD (1974) Chromatin structure: A repeating unit of histones and DNA. Science 184, 868-871.

114. Funke JJ, Ketterer P, Lieleg C, Korber P and Dietz H (2016) Exploring nucleosome unwrapping using DNA origami. Nano Lett. 16, 7891-7898.

115. Funke JJ, Ketterer P, Lieleg C, Schunter S, Korber P and Dietz H (2016) Uncovering the forces between nucleosomes using DNA origami. Sci. Adv. 2, e1600974.

116. Le JV, Luo Y, Darcy MA, Lucas CR, Goodwin MF, Poirier MG and Castro CE (2016) probing nucleosome stability with a DNA origami nanocaliper. ACS Nano 10, 7073-7084.

117. Fernandez JM and Li H (2004) Force-clamp spectroscopy monitors the folding trajectory of a single protein. Science 303 1674-1678.

118. Rief M, Gautel M, Oesterhelt F, Fernandez JM and Gaub HE (1997) Reversible unfolding of individual titin immunoglobulin domains by AFM. Science 276, 1109-1112.

119. Smith SB, Cui Y and Bustamante C (1996) Overstretching B-DNA: the elastic response of individual double-stranded and single-stranded DNA molecules. Science 271, 795-799.

120. Pfitzner E, Wachauf C, Kilchherr F, Pelz B, Shih W M, Rief M and Dietz H (2013) Rigid DNA beams for high-resolution single-molecule mechanics. Angew. Chem. Int. Ed. 52, 7766-7771.

121. Nickels P C, Wünsch B, Holzmeister P, Bae W, Kneer L M, Grohmann D, Tinnefeld P and Liedl T (2016) Molecular force spectroscopy with a DNA origami–based nanoscopic force clamp. Science 354, 305-307.

122. Kilchherr F, Wachauf C, Pelz B, Rief M, Zacharias M and Dietz H (2016) Single-molecule dissection of stacking forces in DNA. Science 353, aaf5508

123. Douglas SM, Chou JJ and Shih WM (2007) DNA-nanotube-induced alignment of membrane proteins for NMR structure determination. Proc. Natl. Acad. Sci. U. S. A. 104, 6644-6648.

124. Bellot G, McClintock MA, Chou JJ and Shih WM (2013) DNA nanotubes for NMR structure determination of membrane proteins. Nat. Protocols 8, 755-770.

125. Berardi MJ, Shih WM, Harrison SC and Chou JJ (2011) Mitochondrial uncoupling protein 2 structure determined by NMR molecular fragment searching. Nature 476, 109-113.

126. Malo J, Mitchell JC, Vénien-Bryan C, Harris JR, Wille H, Sherratt DJ and Turberfield AJ (2005) Engineering a 2D protein–DNA crystal Angew. Chem. Int. Ed. 44, 3057-3061.

127. Selmi DN, Adamson RJ, Attrill H, Goddard AD, Gilbert RJC, Watts A and Turberfield AJ (2011) DNA-templated protein arrays for single-molecule imaging. Nano Lett. 11, 657-660.

128. Fernandez-Leiro R and Scheres SHW (2016) Unravelling biological macromolecules with cryo-electron microscopy. Nature 537, 339-346.

129. Glaeser RM (2016) How good can cryo-EM become? Nat. Meth. 13, 28-32.

130. Bai XC, McMullan G and Scheres SH (2015) How cryo-EM is revolutionizing structural biology. Trends Biochem. Sci. 40, 49-57.

131. Bai XC, Martin TG, Scheres SHW and Dietz H (2012) Cryo-EM structure of a 3D DNA-origami object. Proc. Natl. Acad. Sci. U. S. A. 109, 20012-20017.

132. Martin TG, Bharat TAM, Joerger AC, Bai XC, Praetorius F, Fersht AR, Dietz H and Scheres SHW (2016) Design of a molecular support for cryo-EM structure determination. Proc. Natl. Acad. Sci. U S A. 113, E7456-E7463.

133. Mirkin CA, Letsinger RL, Mucic RC and Storhoff JJ (1996) A DNA-based method for rationally assembling nanoparticles into macroscopic materials. Nature 382, 607-609.

134. Alivisatos AP, Johnsson KP, Peng X, Wilson TE, Loweth CJ, Bruchez MP and Schultz PG (1996) Organization of 'nanocrystal molecules' using DNA. Nature 382, 609-611.

135. Schreiber R, Santiago I, Ardavan A and Turberfield AJ (2016) Ordering gold nanoparticles with DNA origami nanoflowers. ACS Nano 10, 7303-7306.

136. Ding B, Deng Z, Yan H, Cabrini S, Zuckermann RN and Bokor J (2010) Gold nanoparticle self-similar chain structure organized by DNA origami. J. Am. Chem. Soc. 132, 3248-3249.

137. O'Brien MN, Jones MR, Lee B, Mirkin CA (2015) Anisotropic nanoparticle complementarity in DNA-mediated co-crystallization. Nat. Mater. 14, 833-839.

138. Schreiber R, Do J, Roller E-M, Zhang T, Schuller V J, Nickels P C, Feldmann J and Liedl T (2014) Hierarchical assembly of metal nanoparticles, quantum dots and organic dyes using DNA origami scaffolds. Nat. Nanotech. 9, 74-78.

139. Wang ZG, Song C and Ding B (2013), Functional DNA nanostructures for photonic and biomedical applications. Small 9, 2210-2222.

140. Rangnekar A and LaBean TH (2014) Building DNA nanostructures for molecular computation, templated assembly, and biological applications. Acc. Chem. Res. 47, 1778-1788.

141. Pinheiro AV, Han D, Shih WM and Yan H (2011) Challenges and opportunities for structural DNA nanotechnology. Nat. Nanotech. 6, 763-772.

142. Kuzyk A, Schreiber R, Fan ZY, Pardatscher G, Roller EM, Hogele A, Simmel FC, Govorov AO and Liedl T (2012) DNA-based self-assembly of chiral plasmonic nanostructures with tailored optical response. Nature 483, 311-314.

143. Shen X, Song C, Wang J, Shi D, Wang Z, Liu N and Ding B (2012) Rolling up gold nanoparticle-dressed DNA origami into three-dimensional plasmonic chiral nanostructures. J. Am. Chem. Soc. 134, 146-149.

144. Shen X, Asenjo-Garcia A, Liu Q, Jiang Q, García de Abajo FJ, Liu N and Ding B (2013) Three-dimensional plasmonic chiral tetramers assembled by DNA origami. Nano Lett. 13, 2128-2133.

145. Kuzyk A, Schreiber R, Zhang H, Govorov A O, Liedl T and Liu N (2014) Reconfigurable 3D plasmonic metamolecules. Nat. Mater. 13, 862-866.

146. Zhou C, Duan X, Liu N (2015) A plasmonic nanorod that walks on DNA origami. Nature Commun. 6, 8102.

147. Urban MJ, Zhou C, Duan X and Liu N (2015) Optically resolving the dynamic walking of a plasmonic walker couple. Nano Lett. 15, 8392-8396.

148. Tian Y, Zhang Y, Wang T, Xin HL, Li H and Gang O (2016) Lattice engineering through nanoparticle–DNA frameworks. Nature Mater. 15, 654-661.

149. Chandrasekaran AR (2016) DNA-nanoparticle tinkertoys. ChemBioChem 17, 1090-1092.

150. Tian Y, Wang T, Liu W, Xin HL, Li H, Ke Y, Shih WM and Gang O (2015) Prescribed nanoparticle cluster architectures and low-dimensional arrays built using octahedral DNA origami frames. Nat. Nanotech. 10, 637-644.

151. Urban MJ, Dutta PK, Wang P, Duan X, Shen X, Ding B, Ke Y and Liu N (2016) Plasmonic toroidal metamolecules assembled by DNA origami. J. Am. Chem. Soc. 138, 5495-5498.

152. Chen Z, Lan X, Chiu YC, Lu XX, Ni WH, Gao HW, Wang QB (2015) Strong chiroptical activities in gold nanorod dimers assembled using DNA origami templates. ACS Photonics 2, 392-397.

153. Lan X, Chen Z, Dai G, Lu X, Ni W, Wang Q (2013) Bifacial DNA origami-directed discrete, three-dimensional, anisotropic plasmonic nanoarchitectures with tailored optical chirality. J. Am. Chem. Soc. 135, 11441-11444.

154. Lan X, Lu X, Shen C, Ke Y, Ni W, Wang Q (2015) Au nanorod helical superstructures with designed chirality. J. Am. Chem. Soc. 137, 457-462.

155. Thacker VV, Herrmann LO, Sigle DO, Zhang T, Liedl T, Baumberg JJ, Keyser UF (2014) DNA origami based assembly of gold nanoparticle dimers for surface-enhanced Raman scattering. Nat. Commun. 5, 3448.

156. Liu B, Ren S, Xing Y, Teng N, Wang J, Zhu D, Su S, Peng H, Wang L, Wang L and Chao J (2017) A gold-nanoparticle-based SERS reporter that rolls on DNA origami templates. ChemNanoMat 3, 760-763.

157. Heck C, Prinz J, Dathe A, Merk V, Stranik O, Fritzsche W, Kneipp J and Bald I (2017) Gold nanolenses self-assembled by DNA origami. ACS Photonics 4, 1123-1130.

158. Zhan P, Dutta PK, Wang P, Song G, Dai M, Zhao S-X, Wang Z-G, Yin P, Zhang W, Ding B and Ke Y (2017) Reconfigurable three-dimensional gold nanorod plasmonic nanostructures organized on DNA origami tripod. ACS Nano 11, 1172-1179.

159. Zhou C, Duan X, Liu N (2017) DNA-nanotechnology-enabled chiral plasmonics: From static to dynamic. Acc. Chem. Res. DOI: 10.1021/acs.accounts.7b00389.

160. Copp SM, Schultz DE, Swasey S and Gwinn EG (2015) Atomically precise arrays of fluorescent silver clusters: A modular approach for metal cluster photonics on DNA nanostructures. ACS Nano 9, 2303-2310.

161. Ko SH, Du K and Liddle JA (2013) Quantum-dot fluorescence lifetime engineering with DNA origami constructs. Angew. Chem. Int. Ed. 52, 1193-1197.

162. Bui H, Onodera C, Kidwell C, Tan Y, Graugnard E, Kuang W, Lee J, Knowlton WB, Yurke B and Hughes WL (2010) Programmable periodicity of quantum dot arrays with DNA origami nanotubes. Nano Lett. 10, 3367-3372.

163. Steinhauer C, Jungmann R, Sobey T L, Simmel F C and Tinnefeld P (2009) DNA origami as a nanoscopic ruler for super-resolution microscopy. Angew. Chem. Int. Ed. 48, 8870-8873.

164. Lin C, Liu Y and Yan H (2007) Self-assembled combinatorial encoding nanoarrays for multiplexed biosensing. Nano Lett. 7, 507-512.

165. Modi S, Swetha MG, Goswami D, Gupta GD, Mayor S and Krishnan Y (2009) A DNA nanomachine that maps spatial and temporal pH changes inside living cells. Nat. Nanotech. 4, 325-330.

166. Modi S, Nizak C, Surana S, Halder S and Krishnan Y (2013) Two DNA nanomachines map pH changes along intersecting endocytic pathways inside the same cell. Nat. Nanotech. 8, 459-467.

167. Cannon BL, Kellis DL, Davis PH, Lee J, Kuang W, Hughes WL, Graugnard E, Yurke B and Knowlton WB (2015) Excitonic AND logic gates on DNA brick nanobreadboards. ACS Photonics 2, 398-404.

168. Albinsson B, Hannestad JK and Börjesson K (2012) Functionalized DNA nanostructures for light harvesting and charge separation. Coord. Chem. Rev. 256, 2399-2413.

169. Dutta PK, Varghese R, Nangreave J, Lin S, Yan H and Liu Y (2011) DNA-directed artificial light-harvesting antenna. J. Am. Chem. Soc. 133, 11985-11993.

170. Hemmig EA, Creatore C, Wünsch B, Hecker L, Mair P, Parker MA, Emmott S, Tinnefeld P, Keyser UF and Chin AW (2016) programming light-harvesting efficiency using DNA origami. Nano Lett. 16, 2369-2374.

171. Acuna G, Möller F, Holzmeister P, Beater S, Lalkens B and Tinnefeld P (2012) Fluorescence enhancement at docking sites of DNA-directed self-assembled nanoantennas. Science 338, 506-510.

172. Lin C, Jungmann R, Leifer A M, Li C, Levner D, Church GM, Shih WM and Yin P (2012) Submicrometre geometrically encoded fluorescent barcodes self-assembled from DNA. Nat. Chem. 4 832-839.

173. Woehrstein JB, Strauss MT, Ong LL, Wei B, Zhang DY, Jungmann R and Yin P (2017) Sub-100-nm metafluorophores with digitally tunable optical properties self-assembled from DNA Science Adv. 3, e1602128.

174. Sahl SJ, Hell SW and Jakobs S (2017) Fluorescence nanoscopy in cell biology. Nat. Rev. Mol. Cell. Biol. 18, 685-701.

175. Hell SW (2007) Far-field optical nanoscopy. Science 316, 1153-1158.

176. Sharonov A and Hochstrasser RM (2006) Wide-field subdiffraction imaging by accumulated binding of diffusing probes. Proc. Natl. Acad. Sci. U. S. A. 103, 18911-18916.

177. Jungmann R, Steinhauer C, Scheible M, Kuzyk A, Tinnefeld P and Simmel FC (2010) Single-molecule kinetics and super-resolution microscopy by fluorescence imaging of transient binding on DNA origami. Nano Lett. 10, 4756-4761.

178. Derr ND, Goodman BS, Jungmann R, Leschziner AE, Shih WM and Reck-Peterson SL (2012) Tug-of-war in motor protein ensembles revealed with a programmable DNA origami scaffold. Science 338, 662-665.

179. Jungmann R, Avendano MS, Dai M, Woehrstein JB, Agasti SS, Feiger Z, Rodal A and Yin P (2016) Quantitative super-resolution imaging with qPAINT. Nat. Meth. 13, 439-442.

180. Schnitzbauer J, Strauss MT, Schlichthaerle T, Schueder F and Jungmann R (2017) Super-resolution microscopy with DNA-PAINT Nat. Protoc. 12, 1198-1228.

181. Jungmann R, Avendaño MS, Woehrstein JB, Dai M, Shih WM and Yin P (2014) Multiplexed 3D cellular super-resolution imaging with DNA-paint and exchange-paint. Nat. Meth. 11, 313-318.

182. Dai M, Jungmann R and Yin P (2016) Optical imaging of individual biomolecules in densely packed clusters. Nat. Nanotech. 11, 798-807.

183. Salas D, Le Gall A, Fiche J-B, Valeri A, Ke Y, Bron P, Bellot G and Nollmann M (2017) Angular reconstitution-based 3D reconstructions of nanomolecular structures from superresolution light-microscopy images. Proc. Natl. Acad. Sci. U. S. A. 114, 9273-9278.

184. Schmied JJ, Gietl A, Holzmeister P, Forthmann C, Steinhauer C, Dammeyer T and Tinnefeld P (2012) Fluorescence and super-resolution standards based on DNA origami. Nat. Meth. 9, 1133-1134.

185. Schmied JJ, Forthmann C, Pibiri E, Lalkens B, Nickels P, Liedl T and Tinnefeld P (2013) DNA origami nanopillars as standards for three-dimensional superresolution microscopy. Nano Lett. 13, 781-785.

186. Schmied JJ, Raab M, Forthmann C, Pibiri E, Wünsch B, Dammeyer T and Tinnefeld P (2014) DNA origami-based standards for quantitative fluorescence microscopy. Nat. Protoc. 9, 1367-1391.

187. Balzarotti F, Eilers Y, Gwosch KC, Gynnå AH, Westphal V, Stefani FD, Elf J and Hell SW (2017) Nanometer resolution imaging and tracking of fluorescent molecules with minimal photon fluxes. Science 355, 606-612.

188. Schlichthaerle T, Strauss MT, Schueder F, Woehrstein JB and Jungmann R (2016) DNA nanotechnology and fluorescence applications. Curr. Opin. Biotechnol. 39, 41-47.

189. Lee K, Cui Y, Lee L P and Irudayaraj J (2014) Quantitative imaging of single mRNA splice variants in living cells. Nat. Nanotech. 9 474-480.

190. Liu GL, Yin Y, Kunchakarra S, Mukherjee B, Gerion D, Jett SD, Bear DG, Gray JW, Alivisatos AP, Lee LP and Chen FF (2006) A nanoplasmonic molecular ruler for measuring nuclease activity and DNA footprinting. Nat. Nanotech. 1 47-52.

191. Frank J (2017) Advances in the field of single-particle cryo-electron microscopy over the last decade. Nat. Protoc. 12, 209-212.

192. Bartesaghi A, Merk A, Banerjee S, Matthies D, Wu X, Milne JLS and Subramaniam S (2015) 2.2 Å resolution cryo-EM structure of β-galactosidase in complex with a cell-permeant inhibitor. Science 348, 1147-1151.

193. Kühlbrandt W (2014) The resolution revolution. Science 343, 1443-1444.

194. Merk A, Bartesaghi A, Banerjee S, Falconieri V, Rao P, Davis MI, Pragani R, Boxer MB, Earl LA, Milne JL and Subramaniam S (2016) Breaking cryo-EM resolution barriers to facilitate drug discovery. Cell 165, 1698-1707.

195. Khoshouei M, Radjainia M, Baumeister W and Danev R (2017) Cryo-EM structure of haemoglobin at 3.2 A determined with the Volta phase plate. Nat Commun. 8, 16099.

196. Neutze R, Wouts R, van der Spoel D, Weckert E and Hajdu J (2000) Potential for biomolecular imaging with femtosecond X-ray pulses. Nature 406, 752-757.

197. Chapman H N, et al. (2011) Femtosecond X-ray protein nanocrystallography. Nature 470, 73-77.

198. Boutet S, et al (2012) High-resolution protein structure determination by serial femtosecond crystallography. Science 337, 362-364.

199. Johansson LC, Stauch B, Ishchenko A and Cherezov V (2017) A Bright Future for Serial Femtosecond Crystallography with XFELs. Trends Biochem. Sci. 42, 749-762.

200. Chapman H N, et al (2006) Femtosecond diffractive imaging with a soft-X-ray free-electron laser. Nature Physics 2, 839-843.

201. Gaffney KJ and Chapman HN (2007) Imaging atomic structure and dynamics with ultrafast X-ray scattering. Science 316 1444-1448.

202. Chapman H N (2017) Opportunities for Structure Determination Using X-ray Free-electron Laser Pulses. In X-Ray free electron lasers: Applications in materials, chemistry and biology. Eds: Bergmann U, Yachandra V and Yano J. pp 397-417. The Royal Society of Chemistry.

203. Aquila A, et al (2015) The linac coherent light source single particle imaging road map. Struct. Dyn. 2, 041701.

204. Seibert MM, et al (2011) Single mimivirus particles intercepted and imaged with an X-ray laser. Nature 470, 78-81.

205. Ekeberg T, et al. (2015) Three-dimensional reconstruction of the giant mimivirus particle with an x-ray free-electron laser. Phys. Rev Lett. 114, 098102.

206. Ayyer K, et al (2016) Macromolecular diffractive imaging using imperfect crystals. Nature 530, 202-206.

207. Küpper J, et al. (2014) X-ray diffraction from isolated and strongly aligned gas-phase molecules with a free-electron laser. Phys. Rev Lett. 112, 083002.

208. Sayre D and Chapman HN (1995) X-ray microscopy. Acta Cryst. A51, 237-252

209. Xavier PL, Seeman NC and Chapman HN (2017) DNA-assisted flow-aligned single-particle diffractive imaging using XFEL. Manuscript in preparation.

210. Peplow M (2017) The next big hit in molecule Hollywood. Nature, 544 408-410.

211. Shibata M, Nishimasu H, Kodera N, Hirano S, Ando T, Uchihashi T and Nureki O (2017) Real-space and real-time dynamics of CRISPR-Cas9 visualized by high-speed atomic force microscopy. Nat. Commun. 8, 1430.

212. Willner EM, Kamada Y, Suzuki Y, Emura T, Hidaka K, Dietz H, Sugiyama H and Endo M (2017) Single-molecule observation of the photoregulated conformational dynamics of DNA origami nanoscissors. Angew. Chem. Int. Ed. DOI: 10.1002/anie.201708722.

213. Park J, Elmlund H, Ercius P, Yuk JM, Limmer DT, Chen Q, Kim K, Han SH, Weitz DA, Zettl A and Alivisatos AP (2015) 3D structure of individual nanocrystals in solution by electron microscopy. Science 349, 290-295.

214. Chen Q, Smith JM, Park J, Kim K, Ho D, Rasool HI, Zettl A and Alivisatos AP (2013) 3D motion of DNA-Au nanoconjugates in graphene liquid cell electron microscopy. Nano Lett. 13, 4556-4561.

215. Mueller C, Harb M, Dwyer JR and Miller RJD (2013) Nanofluidic cells with controlled pathlength and liquid flow for rapid, high-resolution in situ imaging with electrons. J. Phys. Chem. Lett. 4, 2339-2347.

216. Lee Tin Wah J, David C, Rudiuk S, Baigl D and Estevez-Torres A (2016) Observing and controlling the folding pathway of DNA origami at the nanoscale. ACS Nano 10, 1978-1987.

217. Longchamp JN, Rauschenbach S, Abb S, Escher C, Latychevskaia T, Kern K and Fink HW (2017) Imaging proteins at the single-molecule level. Proc. Natl. Acad. Sci. U. S. A. 114, 1474-1479.

218. Weisenburger S, Boening D, Schomburg B, Giller K, Becker S, Griesinger C and Sandoghdar V (2017) Cryogenic optical localization provides 3D protein structure data with Angstrom resolution. Nat. Meth. 14, 141-144.

219. Dashti A, et al (2014) Trajectories of the ribosome as a Brownian nanomachine. Proc. Natl. Acad. Sci. U. S. A. 111, 17492-17497.

220. Frank J (2017) Time-resolved cryo-electron microscopy: Recent progress. J. Struct. Biol. DOI: 10.1016/j.jsb.2017.06.005.

221. Hosseinizadeh A et al (2017) Conformational landscape of a virus by single-particle X-ray scattering. Nat. Meth. 14, 877-881.

222. Kurta RP et al (2017) Correlations in scattered X-ray laser pulses reveal nanoscale structural features of viruses. Phys. Rev Lett. 119, 158102.

223. Schneider R et al (2017) Quantum imaging with incoherently scattered light from a free-electron laser. Nature Physics DOI:10.1038/nphys4301.

224. Classen A, Ayyer K, Chapman H N, Röhlsberger R and von Zanthier J (2017) Incoherent diffractive imaging via intensity correlations of hard X rays. Phys. Rev Lett. 119, 053401.

225. Lorenz UJ and Zewail AH (2013) Biomechanics of DNA structures visualized by 4D electron microscopy. Proc. Natl. Acad. Sci. U. S. A. 110, 2822-2827.

226. Pande K et al (2016) Femtosecond structural dynamics drives the trans/cis isomerization in photoactive yellow protein. Science 352, 725-729.

227. Kärtner F X, et al (2016) AXSIS: Exploring the frontiers in attosecond X-ray science, imaging and spectroscopy. Nuclear Instruments and Methods in Physics Research Section A: Accelerators, Spectrometers, Detectors and Associated Equipment 829, 24-29.

228. Fischer S, Hartl C, Frank K, Rädler JO, Liedl T and Nickel B (2016) Shape and interhelical spacing of DNA origami nanostructures studied by small-angle X-ray scattering. Nano Lett. 16, 4282-4287.

229. Bruetzel LK, Gerling T, Sedlak SM, Walker PU, Zheng W, Dietz H and Lipfert J (2016) Conformational changes and flexibility of DNA devices observed by small-angle X-ray scattering. Nano Lett. 16, 4871-4879.

230. Nicoli F, Barth A, Bae W, Neukirchinger F, Crevenna AH, Lamb DC and Liedl T (2017) Directional photonic wire mediated by homo-förster resonance energy transfer on a DNA origami platform ACS Nano, DOI: 10.1021/acsnano.7b05631.

231. Cheng RKY, Abela R and Hennig M (2017) X-ray free electron laser: opportunities for drug discovery. Essays In Biochemistry 61, 529-542.

232. de la Cruz MJ, Hattne J, Shi D, Seidler P, Rodriguez J, Reyes FE, Sawaya MR, Cascio D, Weiss SC, Kim SK, Hinck CS, Hinck AP, Calero G, Eisenberg D and Gonen T (2017) Atomic-resolution structures from fragmented protein crystals with the cryoEM method MicroED. Nat. Meth. 14, 399-402.

233. Chapman HN, Yefanov OM, Ayyer K, White TA, Barty A, Morgan A, Mariani V, Oberthuer D and Pande K (2017) Continuous diffraction of molecules and disordered molecular crystals. J. Appl. Crystallogr. 50, 1084-1103.

234. Wei X, Nangreave J and Liu Y (2014) Uncovering the self-assembly of DNA nanostructures by thermodynamics and kinetics. Acc. Chem. Res. 47, 1861-1870.

235. Dunn KE, Dannenberg F, Ouldridge TE, Kwiatkowska M, Turberfield AJ and Bath J (2015) Guiding the folding pathway of DNA origami. Nature. 525, 82-86.

236. Marras AE, Zhou L, Kolliopoulos V, Su HJ and Castro CE (2016) Directing folding pathways for multi-component DNA origami nanostructures with complex topology. New J. Phys. 18, 055005.

237. Li W, Yang Y, Jiang S, Yan H and Liu Y (2014) Controlled nucleation and growth of DNA tile arrays within prescribed DNA origami frames and their dynamics. J. Am. Chem. Soc. 136, 3724-3727.

238. Pound E, Ashton JR, Becerril HA and Woolley AT (2009) Polymerase chain reaction based scaffold preparation for the production of thin, branched DNA origami nanostructures of arbitrary sizes. Nano Lett. 9, 4302-4305.

239. Zhang H, Chao J, Pan D, Liu H, Huang Q and Fan C (2012) Folding super-sized DNA origami with scaffold strands from long-range PCR. Chem. Commun. 48, 6405-6407.

240. Said H, Schuller VJ, Eber FJ, Wege C, Liedl T and Richert C (2013) M1.3 - a small scaffold for DNA origami. Nanoscale 5, 284-290.

241. Erkelenz M, Bauer DM, Meyer R, Gatsogiannis C, Raunser S, Saccà B and Niemeyer CM (2014) A facile method for preparation of tailored scaffolds for DNA-origami. Small 10, 73-77.

242. Marchi AN, Saaem I, Vogen BN, Brown S and LaBean TH (2014) Toward larger DNA origami. Nano Lett. 14, 5740-5747.

243. Chandrasekaran AR, Pushpanathan M and Halvorsen K (2016) Evolution of DNA origami scaffolds. Mat. Lett. 170, 221-224.

244. Sobczak JP, Martin TG, Gerling T and Dietz H (2012) Rapid folding of DNA into nanoscale shapes at constant temperature. Science 338, 1458-1461.

245. Jungmann R, Liedl T, Sobey TL, Shih W and Simmel FC (2008) Isothermal assembly of DNA origami structures using denaturing agents. J. Am. Chem. Soc. 130, 10062-10063.

246. Song J, Zhang Z, Zhang S, Liu L, Li Q, Xie E, Gothelf KV, Besenbacher F and Dong M (2013) Isothermal hybridization kinetics of DNA assembly of two-dimensional DNA origami. Small 9, 2954-2959.

247. Myhrvold C, Dai M, Silver PA, Yin P (2013) Isothermal self-assembly of complex DNA structures under diverse and biocompatible conditions. Nano Lett. 13, 4242-4248.

248. Zhang Z, Song J, Besenbacher F, Dong M, Gothelf KV (2013) Self-assembly of DNA origami and single-stranded tile structures at room temperature. Angew. Chem. Int. Ed. 52, 9219-9223.

249. Kopielski A, Schneider A, Csáki A, Fritzsche W (2015) Isothermal DNA origami folding: avoiding denaturing conditions for one-pot, hybrid-component annealing. Nanoscale 7, 2102-2106.

250. Ducani C, Kaul C, Moche M, Shih WM and Hogberg B (2013) Enzymatic production of 'monoclonal stoichiometric' single-stranded DNA oligonucleotides. Nat. Meth. 10, 647-652.

251. Niekamp S, Blumer K, Nafisi PM, Tsui K, Garbutt J, Douglas SM (2016) Folding complex DNA nanostructures from limited sets of reusable sequences. Nucleic Acids Res. 44, e102.

252. Saaem I, Ma KS, Marchi AN, LaBean TH, Tian J (2010) In situ synthesis of DNA microarray on functionalized cyclic olefin copolymer substrate. ACS Appl. Mater. Interfaces 2, 491-497.

253. Marchi AN, Saaem I, Tian J, LaBean TH (2013) One-pot assembly of a hetero-dimeric DNA origami from chip-derived staples and double-stranded scaffold. ACS Nano 7, 903-910.

254. Schmidt TL, Beliveau BJ, Uca YO, Theilmann M, Da Cruz F, Wu CT, Shih WM (2015) Scalable amplification of strand subsets from chip-synthesized oligonucleotide libraries. Nat. Commun. 6, 8634.

255. Nickels PC, Ke Y, Jungmann R, Smith DM, Leichsenring M, Shih WM, Liedl T and Högberg B (2014) DNA origami structures directly assembled from intact bacteriophages. Small 10, 1765-1769.

256. Praetorius F, Kick B, Behler KL, Honemann MN, Weuster-Botz D and Dietz H (2017) Biotechnological mass-production of DNA origami. Nature, In press.

257. Mathur D and Medintz IL (2017) Analyzing DNA nanotechnology: A call to arms for the analytical chemistry community. Anal. Chem. 89, 2646-2663.

258. Lin C, Perrault SD, Kwak M, Graf F and Shih WM (2013) Purification of DNA-origami nanostructures by rate-zonal centrifugation. Nucl. Acids Res. 41, e40.

259. Shaw A, Benson E and Högberg B (2015) Purification of functionalized DNA origami nanostructures. ACS Nano 9, 4968-4975.

260. Stahl E, Martin TG, Praetorius F and Dietz H (2014) Facile and scalable preparation of pure and dense DNA origami solutions. Angew. Chem., Int. Ed. 53, 12735-12740.

261. Wickham SFJ, Endo M, Katsuda Y, Hidaka K, Bath J, Sugiyama H and Turberfield AJ (2011) Direct observation of stepwise movement of a synthetic molecular transporter. Nat. Nanotech. 6, 166-169.

262. Douglas SM, Bachelet I and Church GM (2012) A logic-gated nanorobot for targeted transport of molecular payloads. Science 335, 831-834.

263. Halvorsen K, Kizer ME, Wang X, Chandrasekaran AR and Basanta-Sanchez M (2017) Shear dependent LC purification of an engineered DNA nanoswitch and implications for DNA origami. Anal Chem. 89, 5673-5677.

264. Timm C and Niemeyer CM (2015), Assembly and purification of enzyme-functionalized DNA origami structures. Angew. Chem. Int. Ed. 54, 6745-6750.

265. Bellot G, McClintock MA, Lin C and Shih WM (2011) Recovery of intact DNA nanostructures after agarose gel-based separation. Nat. Methods 8, 192-194.

266. Marth G, Hartley AM, Reddington SC, Sargisson LL, Parcollet M, Dunn KE, Jones DD and Stulz E (2017) Precision templated bottom-up multiprotein nanoassembly through defined click chemistry linkage to DNA. ACS Nano 11, 5003-5010.

267. Valsangkar V, Chandrasekaran AR, Wang R, Haruehanroengra P, Levchenko O, Halvorsen K and Sheng J (2017) Click-based functionalization of a 2'-O-propargyl-modified branched DNA nanostructure. J. Mater. Chem. B 5, 2074-2077.

268. Rusling DA and Fox KR (2014) Sequence-specific recognition of DNA nanostructures. Methods 67, 123-133.

269. Chandrasekaran AR and Rusling DA (2017) Triplex-forming oligonucleotides: a third strand for DNA nanotechnology. Nucleic Acids Res. DOI: 10.1093/nar/gkx1230.

270. Taylor AI, Beuron F, Peak-Chew SY, Morris EP, Herdewijn P and Holliger P (2016) Nanostructures from synthetic genetic polymers. Chembiochem 17, 1107-1110.

271. Georgiadis MM, Singh I, Kellett WF, Hoshika S, Benner SA and Richards NG (2015) Structural basis for a six nucleotide genetic alphabet. J. Am. Chem. Soc. 137, 6947-6955.

272. Malyshev DA, Dhami K, Lavergne T, Chen T, Dai N, Foster JM, Corrêa IR Jr and Romesberg FE (2014) A semi-synthetic organism with an expanded genetic alphabet. Nature 509, 385-388.

273. Liu Q, Liu G, Wang T, Fu J, Li R, Song L, Wang ZG, Ding B, Chen F (2017) Enhanced stability of DNA nanostructures by incorporation of unnatural base pairs. ChemPhysChem DOI: 10.1002/cphc.201700809.

274. Grabow WW and Jaeger L (2014) RNA self-assembly and RNA nanotechnology. Acc. Chem. Res. 47, 1871-1880.

275. Sparvath SL, Geary CW and Andersen ES (2017) 3D DNA nanostructure: Methods and protocols, Eds: Ke Y and Wang P (New York, NY: Springer New York) pp 51-80.

276. Chevalier A et al (2017) Massively parallel de novo protein design for targeted therapeutics. Nature 550, 74-79.

277. Liu Y, Gonen S, Gonen T and Yeates T (2017) Near-atomic cryo-EM imaging of a small protein displayed on a designed scaffolding system. bioRxiv 212233; DOI: https://doi.org/10.1101/212233.

278. Hahn J, Wickham SFJ, Shih WM and Perrault SD (2014) Addressing the instability of DNA nanostructures in tissue culture. ACS Nano 8, 8765-8775.

279. Ponnuswamy N, Bastings MMC, Nathwani B, Ryu JH, Chou LYT, Vinther M, Li WA, Anastassacos FM, Mooney DJ and Shih WM (2017) Oligolysine-based coating protects DNA nanostructures from low-salt denaturation and nuclease degradation. Nature Commun. 8, 15654.

280. Jiang Q, Song C, Nangreave J, Liu X, Lin L, Qiu D, Wang ZG, Zou G, Liang X, Yan H and Ding B (2012) DNA origami as a carrier for circumvention of drug resistance. J. Am. Chem. Soc. 134, 13396-133403.

281. Schuller VJ, Heidegger S, Sandholzer N, Nickels PC, Suhartha NA, Endres S, Bourquin C and Liedi T (2011) Cellular immunostimulation by CpG-sequence-coated DNA origami structures. ACS Nano 5, 9696-9702.

282. Lee H, et al. (2012) Molecularly self-assembled nucleic acid nanoparticles for targeted in vivo siRNA delivery. Nat. Nanotech. 7, 389-393.

283. Ora A, Järvihaavisto E, Zhang H, Auvinen H, Santos HA, Kostiainen MA and Linko V (2016). Cellular delivery of enzyme-loaded DNA origami. Chem. Commun. 52, 14161-14164.

284. Huang Y, Huang W, Chan L, Zhou B, Chen T (2016) A multifunctional DNA origami as carrier of metal complexes to achieve enhanced tumoral delivery and nullified systemic toxicity. Biomaterials 103, 183-196.

285. Hansen CH, Yang D, Koussa MA and Wong WP (2017) Nanoswitch-linked immunosorbent assay (NLISA) for fast, sensitive, and specific protein detection. Proc. Natl. Acad. Sci. U. S. A. 114, 10367-10372.

286. Chandrasekaran AR, Zavala J, Halvorsen K (2016) Programmable DNA nanoswitches for detection of nucleic acid sequences. ACS Sens. 1, 120-123.

287. Robinson BH and Seeman NC (1987) The design of a biochip: a self-assembling molecular-scale memory device. Protein Eng. 1, 295-300.

288. Kershner RJ, et al. (2009) Placement and orientation of individual DNA shapes on lithographically patterned surfaces. Nat. Nanotech. 4, 557-561.

289. Gopinath A, Miyazono E, Faraon A, Rothemund PW. (2016) Engineering and mapping nanocavity emission via precision placement of DNA origami. Nature 535, 401-405.

290. Jin Z, Sun W, Ke Y, Shih CJ, Paulus GL, Wang QH, Mu B, Yin P and Strano MS (2013) Metallized DNA nanolithography for encoding and transferring spatial information for graphene patterning. Nat. Commun. 4, 1663.

291. He X, Sha R, Zhuo R, Mi Y, Chaikin PM and Seeman NC (2017) Exponential growth and selection in self-replicating materials from DNA origami rafts. Nature Mater. 16, 993-997.

292. Ketterer P, Willner EM and Dietz H (2016) Nanoscale rotary apparatus formed from tight-fitting 3D DNA components. Science Adv. 2, e1501209.

293. Song J, Li Z, Wang P, Meyer T, Mao C and Ke Y (2017) Reconfiguration of DNA molecular arrays driven by information relay. Science 357, eaan3377.

294. Marras AE, Zhou L, Su HJ, Castro CE (2015) Programmable motion of DNA origami mechanisms. Proc. Natl. Acad. Sci. U. S. A. 112 713-718.

295. Czogalla A, Franquelim HG and Schwille P (2016) DNA nanostructures on membranes as tools for synthetic biology. Biophys. J. 110, 1698-1707.

296. Qian L and Winfree E (2011) Scaling up digital circuit computation with DNA strand displacement cascades. Science 332, 1196-1201.

297. Adleman LM (1994) Molecular computation of solutions to combinatorial problems. Science 266, 1021-1024.

298. Chandrasekaran AR, Levchenko O, Patel DS, MacIsaac M and Halvorsen K (2017) Addressable configurations of DNA nanostructures for rewritable memory. Nucl. Acids Res. 45, 11459-11465.

299. Church GM, Gao Y and Kosuri S (2012) Next-generation digital information storage in DNA. Science 337, 1628-1628.

300. Yazdi SMHT, Yuan Y, Ma J, Zhao H and Milenkovic O (2015) A rewritable, random-access DNA-based storage system. Sci. Rep. 5, 14138.

301. Bornholt J, Lopez R, Carmean DM, Ceze L, Seelig G Strauss K (2017) Toward a DNA-based archival storage system. IEEE Micro, 37, 98-104, 2017.

302. Shipman SL, Nivala J, Macklis JD, Church GM (2017) CRISPR-Cas encoding of a digital movie into the genomes of a population of living bacteria. Nature 547, 345-349.

303. Erlich Y, Zielinski D (2017) DNA Fountain enables a robust and efficient storage architecture. Science 355, 950-954.

304. Winfree E, Liu F, Wenzler LA and Seeman NC (1998) Design and self-assembly of two-dimensional DNA crystals. Nature 394, 539-544.

305. Ke Y, Douglas SM, Liu M, Sharma J, Cheng A, Leung A, Liu Y, Shih WM and Yan H (2009) Multilayer DNA origami packed on a square lattice. J. Am. Chem. Soc. 131, 15903-15908.

306. Linko V, Eerikäinen M, Kostiainen MA (2015) A modular DNA origami-based enzyme cascade nanoreactor. Chem. Commun. 51, 5351-5354.

307. Jiang Q, Shi Y, Zhang Q, Li N, Zhan P, Song L, Dai L, Tian J, Du Y, Cheng Z and Ding B (2015) A self-assembled DNA origami-gold nanorod complex for cancer theranostics. Small 11, 5134-5141.

308. Majumder U, Rangnekar A, Gothelf KV, Reif JH and LaBean TH (2011) Design and construction of double-decker tile as a route to three-dimensional periodic assembly of DNA. J. Am. Chem. Soc. 133, 3843-3845.

309. Zheng J, Constantinou PE, Micheel C, Alivisatos AP, Kiehl RA and Seeman NC (2006) Two-dimensional nanoparticle arrays show the organizational power of robust DNA motifs. Nano Lett. 6, 1502-1504.

310. He Y, Chen Y, Liu H, Ribbe AE and Mao C (2005) Self-assembly of hexagonal DNA two-dimensional (2D) arrays. J. Am. Chem. Soc. 127, 12202-12203.

311. He Y, Tian Y, Chen Y, Deng Z, Ribbe AE and Mao C (2005) Sequence symmetry as a tool for designing DNA nanostructures. Angew. Chem. Int. Ed. 44, 6694-6696.

312. He Y, Tian Y, Ribbe AE and Mao C (2006) Highly connected two-dimensional crystals of DNA six-point-stars. J. Am. Chem. Soc. 128, 15978-15979.

313. Kuzuya A, Kimura M, Numajiri K, Koshi N, Ohnishi T, Okada F, Komiyama M (2009) Precisely programmed and robust 2D streptavidin nanoarrays by using periodical nanometer-scale wells embedded in DNA origami assembly. Chembiochem. 10, 1811-1815.

314. Voigt NV, Torring T, Rotaru A, Jacobsen MF, Ravnsbaek JB, Subramani R, Mamdouh W, Kjems J, Mokhir A, Besenbacher F and Gothelf KV (2010) Single-molecule chemical reactions on DNA origami. Nat. Nanotech. 5, 200-203.

315. Yan H, Park SH, Finkelstein G, Reif JH and LaBean TH (2003) DNA-templated self-assembly of protein arrays and highly conductive nanowires. Science 301, 1882-1884.

316. Nakata E, Liew FF, Uwatoko C, Kiyonaka S, Mori Y, Katsuda Y, Endo M, Sugiyama H and Morii T (2012) Zinc-finger proteins for site-specific protein positioning on DNA-origami structures. Angew. Chem. Int. Ed. 51, 2421-2424.

317. Chhabra R, Sharma J, Ke Y, Liu Y, Rinker S, Lindsay S and Yan H (2007) Spatially addressable multiprotein nanoarrays templated by aptamer-tagged DNA nanoarchitectures. J. Am. Chem. Soc. 129, 10304-10305.

318. Udomprasert A, Bongiovanni MN, Sha R, Sherman WB, Wang T, Arora PS, Canary JW, Gras SL and Seeman NC (2014) Amyloid fibrils nucleated and organized by DNA origami constructions. Nat. Nanotech. 9, 537-541.

319. Jusuk I, Vietz C, Raab M, Dammeyer T and Tinnefeld P (2015) Super-resolution imaging conditions for enhanced yellow fluorescent protein (eYFP) demonstrated on DNA origami nanorulers Sci. Rep. 5, 14075.

320. Ke Y, Meyer T, Shih WM and Bellot G (2016) Regulation at a distance of biomolecular interactions using a DNA origami nanoactuator. Nat. Commun. 7, 10935.

321. Sacca B, Meyer R, Erkelenz M, Kiko K, Arndt A, Schroeder H, Rabe KS and Niemeyer CM (2010) Orthogonal protein decoration of DNA origami. Angew. Chem. Int. Ed. 49, 9378-9383.

322. Schiffels D, Szalai VA and Liddle JA (2017) Molecular precision at micrometer length scales: hierarchical assembly of DNA-protein nanostructures. ACS Nano 11, 6623-6629.

323. Sprengel A, et al (2017) Tailored protein encapsulation into a DNA host using geometrically organized supramolecular interactions. Nat. Commun. 8, 14472.

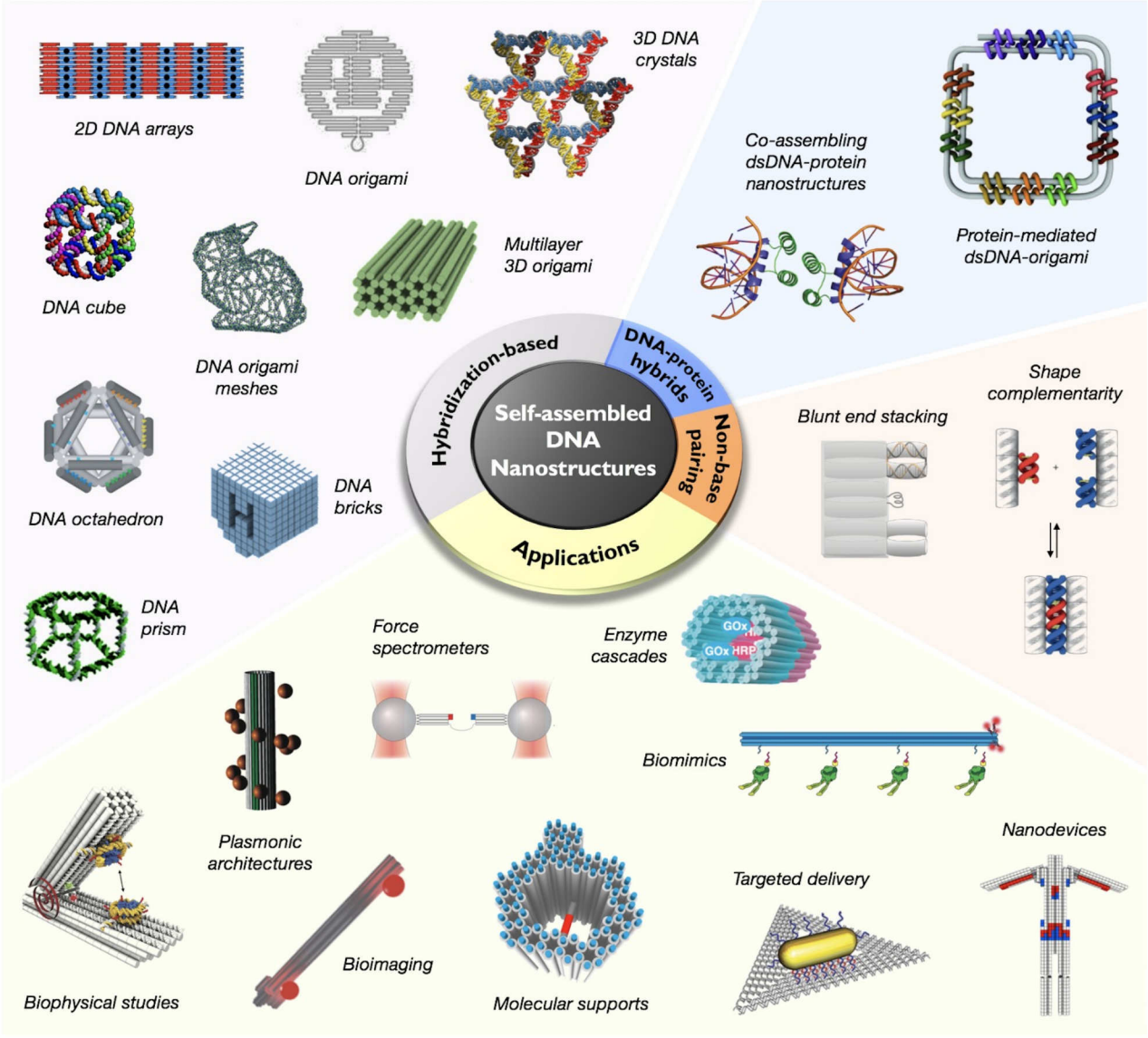

Figure 1. *Overview of DNA nanotechnology.* Illustration shows different assembly types (hybridization-based, protein-DNA association and blunt end stacking/shape complementary based assembly) and representative examples of various applications. Images reproduced with permission from the following references: [3, 20, 39, 52, 58, 72, 78, 304] Copyright 2003, 2004, 2009, 2006, 2015, 2011, 2015, 1998 respectively: Nature Publishing Group (NPG); [26, 143, 305] Copyright 2007, 2012, 2009 respectively: American Chemical Society (ACS); [63, 73, 79, 115, 122, 178, 186] Copyright 2012, 2015, 2017, 2016, 2016, 2012, 2011 respectively: American Association for the Advancement of Science (AAAS); [306] Copyright 2015, Royal Society of Chemistry (RSC); [132] Copyright 2016, National Academy of Sciences (NAS); [307] Copyright 2015, WILEY-VCH.

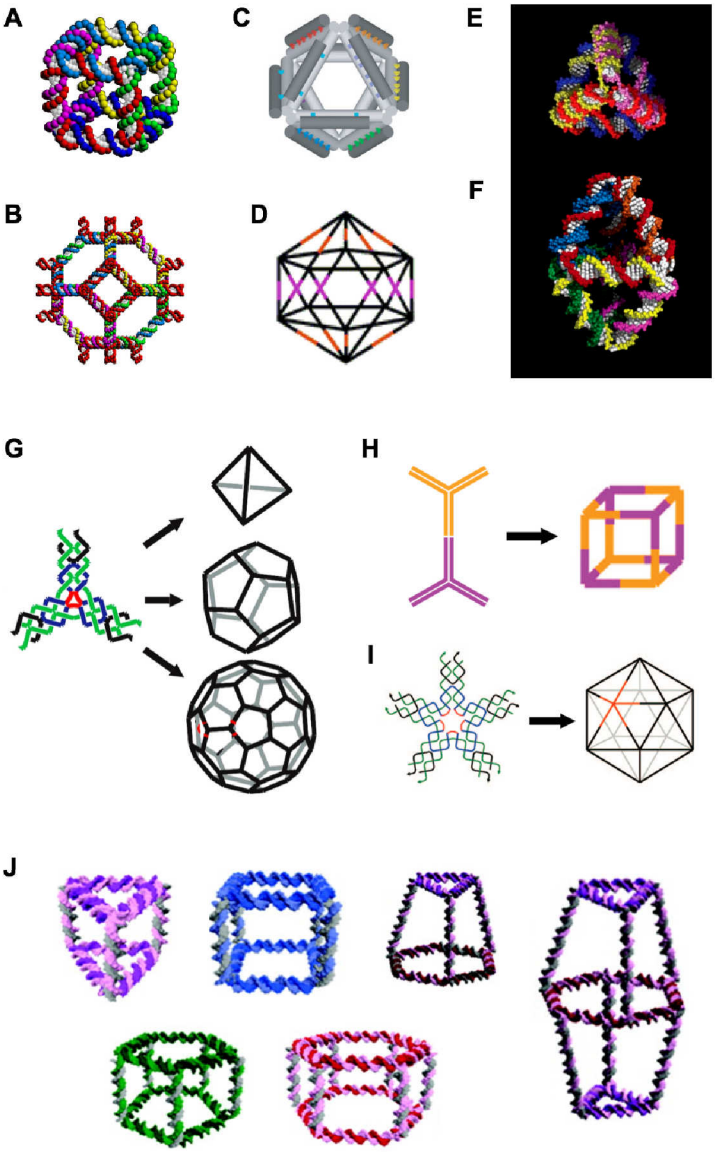

Figure 2. *DNA wire-frame objects.* (A) DNA cube [18], (B) truncated octahedron [19], (C) octahedron [20], (D) icosahedron [21], (E) tetrahedron [22], (F) double tetrahedron [22], (G) tetrahedron, octahedron and bucky ball assembled from a three-point-star motif [23], (H) cube assembled from three-point-star motif [24], (I) icosahedron assembled from a five-point-star motif [25], (J) representative examples of DNA prisms [26]. Images reproduced with permission from the following references: [3, 20, 22, 23] Copyright 2003, 2004, 2008, 2008: NPG; [19, 24, 26] Copyright 1994, 2009, 2007: ACS; [21] Copyright 2009, WILEY-VCH; [25] Copyright 2016, NAS.

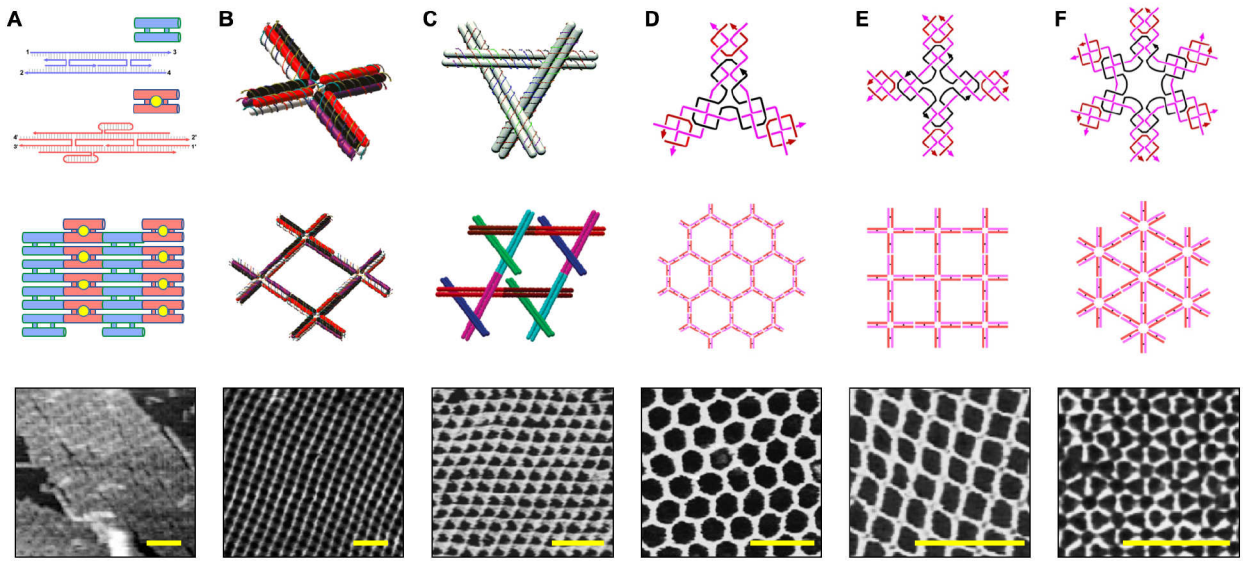

Figure 3. *Two-dimensional DNA arrays.* (A) A double crossover (DX) based alternating array [304]. The A and B tiles alternate in the array and are connected via sticky ends. The B tile has a hairpin (yellow circle) as a topological marker to identify the two types of tiles. (B) A cross-shaped double-decker tile [308] (C) A tensegrity triangle with double crossover edges [309] (D) a three-point-star motif where each arm is a four-way junction [310], (E) a four-point-star (cross) motif [311], (F) a six-point-star motif [312]. AFM images for each type of array is shown in the bottom panel. Images reproduced with permission from the following references: [304] Copyright 1998: NPG; [308, 309, 310, 312] Copyright 2011, 2006, 2005, 2006: ACS; [311] Copyright 2005, WILEY-VCH.

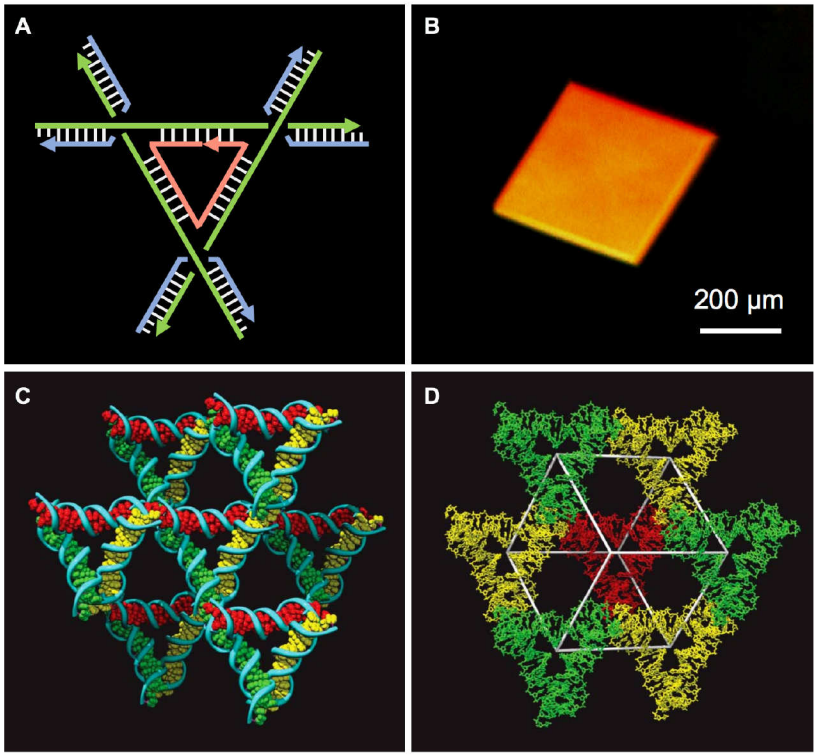

Figure 4. *Designed DNA crystals.* (A) A two helical turn tensegrity triangle motif that assembled into a three-dimensional lattice, (B) the crystal formed from such a motif (C) assembly of triangles into a rhombohedral lattice, the three different directions are shown in three colors (D) the crystals structure showing triangle arrangement in the crystal, the white box shows the rhombohedral cavity formed within 8 such triangles. Images adapted and reproduced from [39] Copyright 2009: NPG.

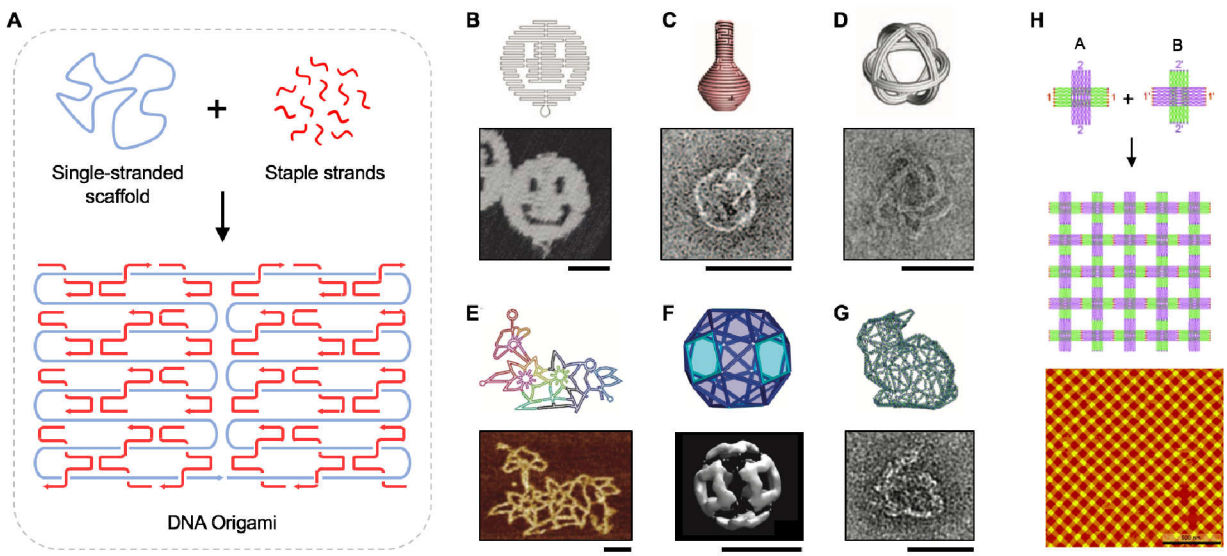

Figure 5. *DNA origami structures.* (A) The method of DNA origami where a long single stranded scaffold is folded into a specific shape by short complementary staple strands. Some examples of objects made using DNA origami: (B) a smiley face [52], (C) a hollow flask [56], (D) a wireframe object [54], (E) a 2D pattern of flowers and a bird [57], (F) a snub cube [57], (G) a nanoscale bunny [58]. (H) A cross-shaped DNA origami yield crystalline 2D DNA arrays [59]. Images reproduced with permission from the following references: [52, 57, 58] Copyright 2006, 2015, 2015: NPG; [53, 56] Copyright 2009, 2011: AAAS; [59] Copyright 2011, WILEY-VCH.

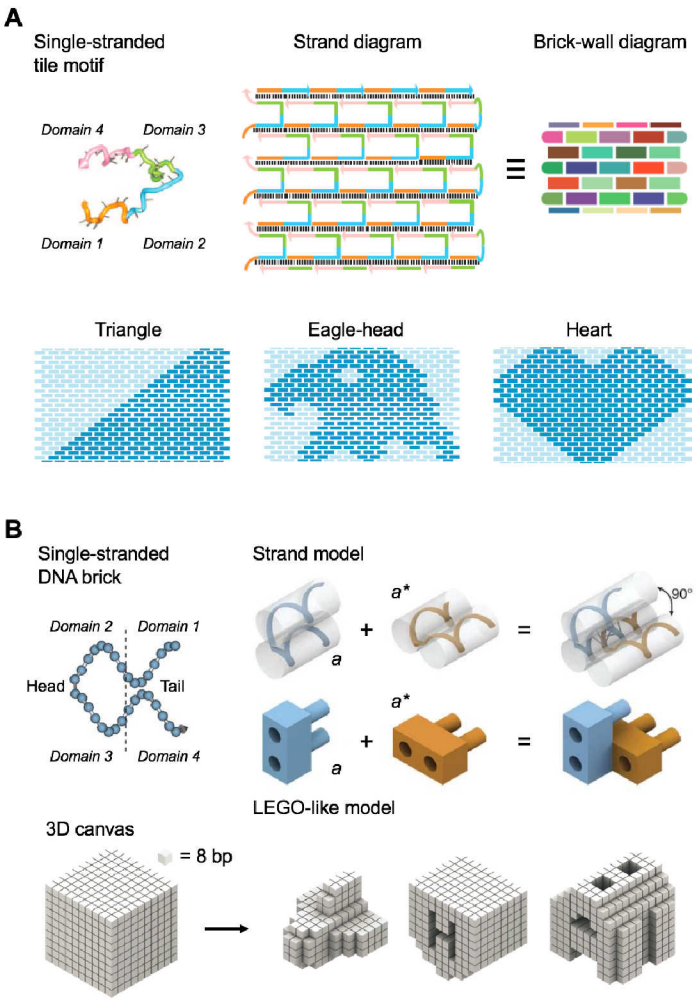

Figure 6. *Alternative methods of large scale assembly.* (A) The molecular canvas strategy where selective single stranded DNA tiles from a pool of tiles assemble to form the specific pattern [62]. (B) The DNA brick strategy to create lego-like building blocks [63]. Images reproduced with permission from the following references: [62] Copyright 2012: NPG; [63] Copyright 2012: AAAS.

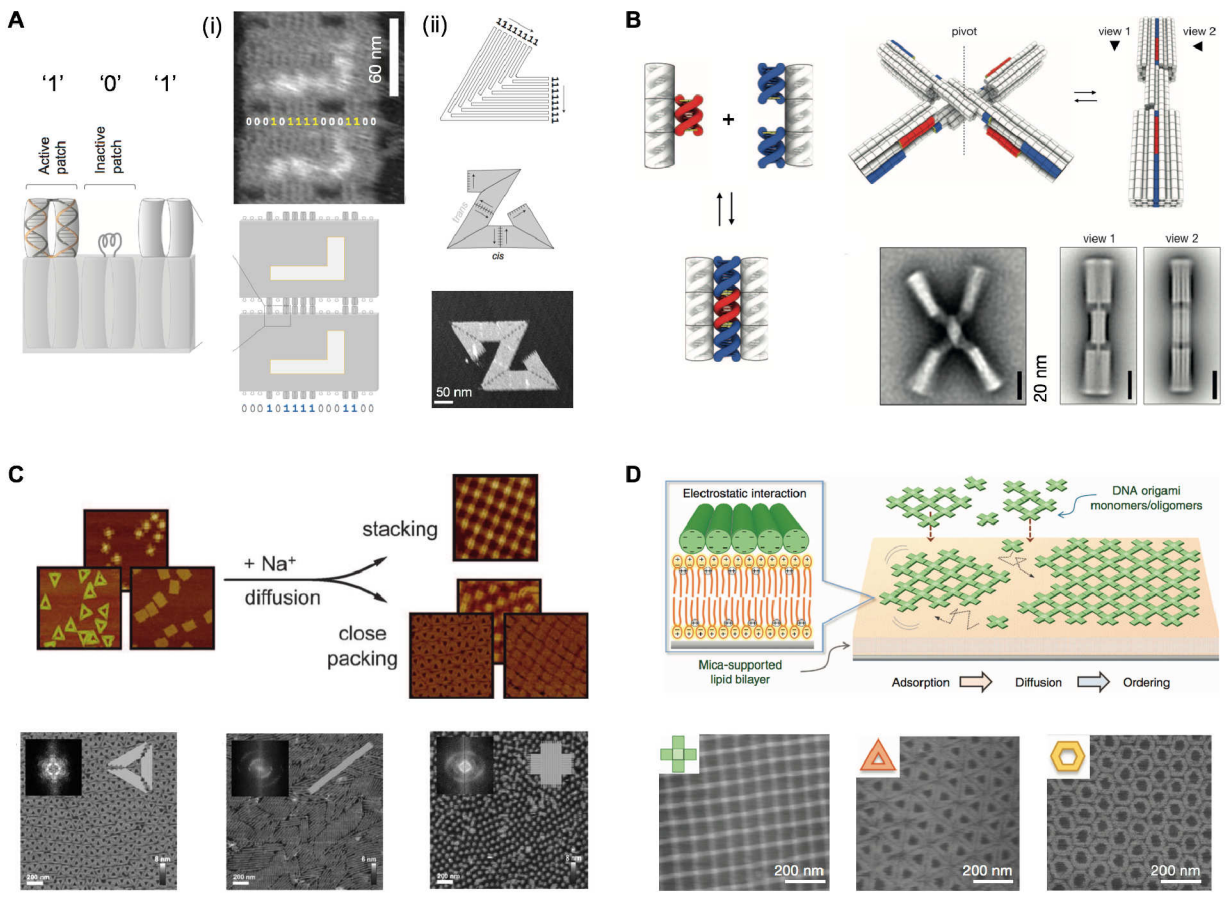

Figure 7. *Non-base pairing assembly.* (A) Blunt end stacking and shape complementarity yield assembly of origami patterns [72], (B) A shape complementary nanodevice [73], (C) Surface-assisted assembly of 2D DNA origami lattices by stacking or close packing interactions in the presence of monovalent ions [75], (D) Membrane-assisted formation of 2D DNA origami lattices via blunt end stacking [77]. Images reproduced with permission from the following references: [72, 77] Copyright 2011, 2015: NPG; [73] Copyright 2015: AAAS; [75] Copyright 2014, WILEY-VCH.

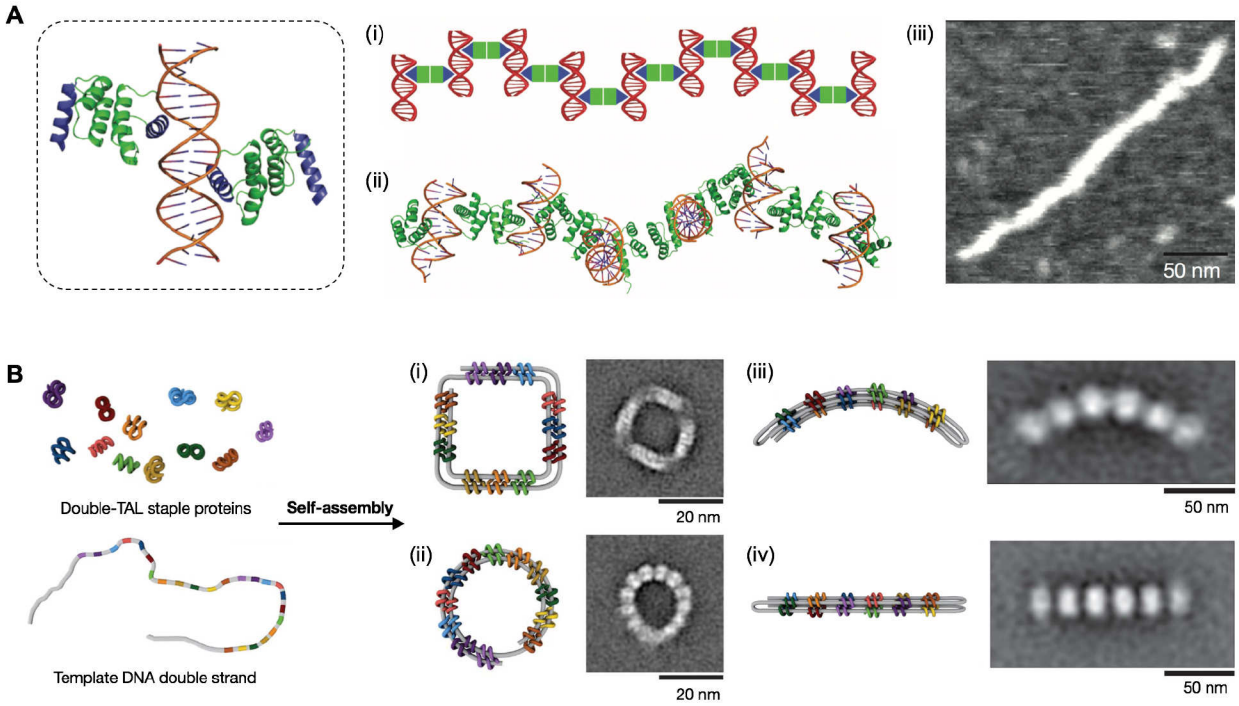

Figure 8. *Protein-assisted assembly of DNA nanostructures.* (A) A protein nanowire [78] (B) An origami strategy involving a double stranded DNA scaffold and proteins as staples, forming a variety of nanostructures (i-iv) [79]. Images reproduced with permission from the following references: [78] Copyright 2015: NPG; [79] Copyright 2017: AAAS.

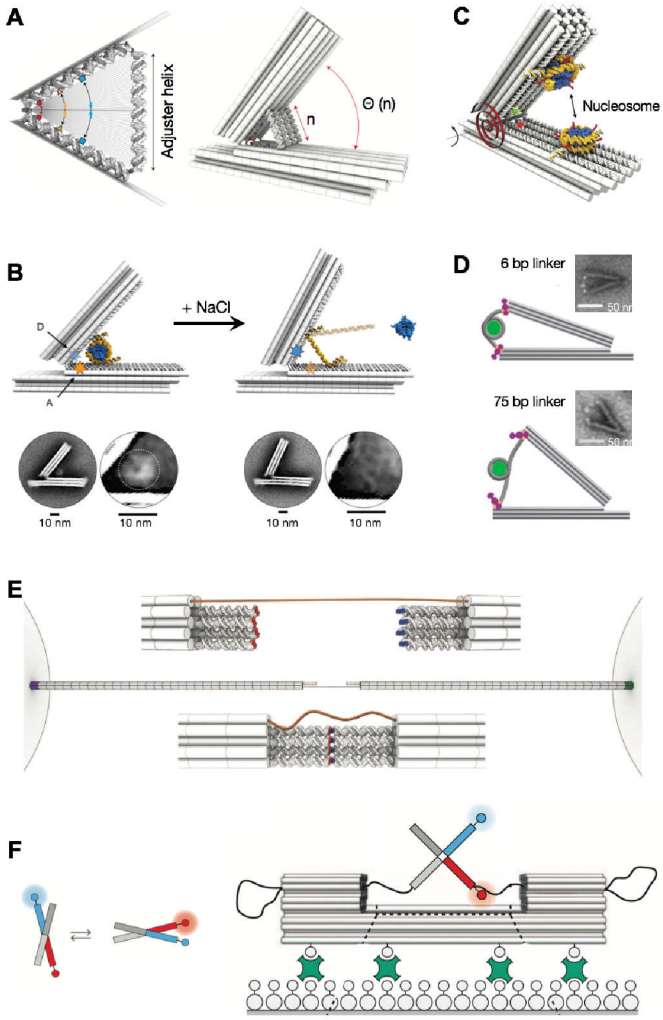

Figure 9. *DNA nanostructures for biophysical analysis.* (A) A DNA origami hinged object that can place molecules in specific distances on the two arms of the hinge [112]. (B) The hinged DNA origami used to explore nucleosome unwrapping [114] (C) A similar DNA origami object used to study the forces between two nucleosomes [115] (D) A DNA origami nanocaliper used to study nucleosome stability [116] (E) DNA origami beams tethered on micrometer sized beads to study base stacking forces [122] (F) DNA origami based force clamps to study Holliday junction conformation [121]. Images reproduced with permission from the following references: [112] Copyright 2016: NPG; [114, 116] Copyright 2016: ACS; [115, 121, 122] Copyright 2016: AAAS.

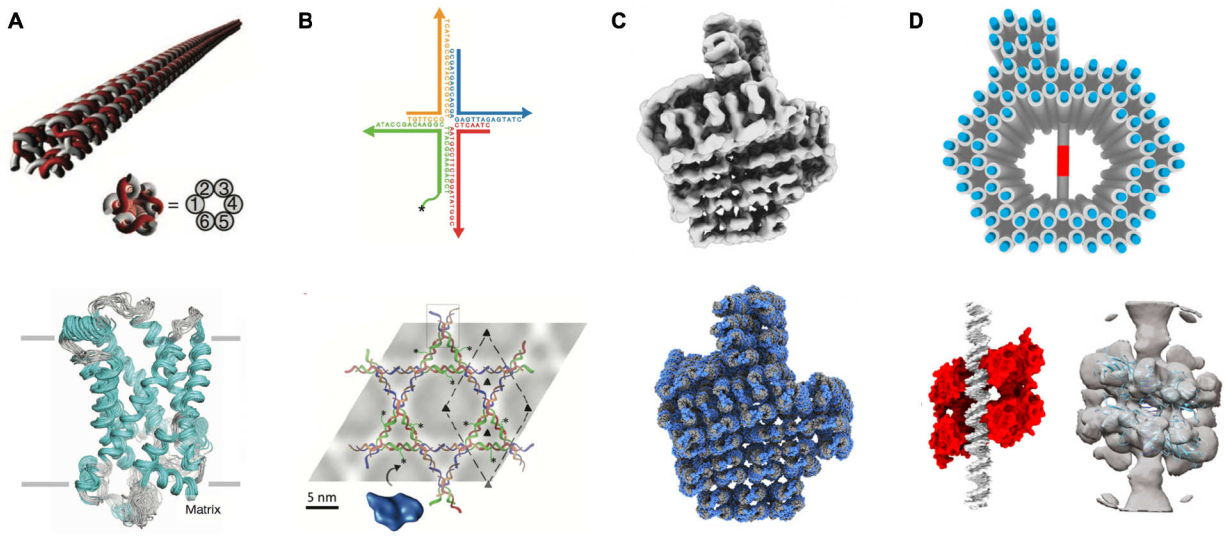

Figure 10. *DNA-based nanostructures and scaffolds for macromolecular structure determination.* (A) DNA nanotubes for aligning proteins for NMR analysis (top) [123] and structure of a mitochondrial uncoupling protein solved using DNA nanotubes [125] (B) DNA junction based 2D arrays to host protein for cryo-EM studies [127]. (C) Cryo EM structure of a 3D DNA origami object [131] (D) A DNA origami-based molecular support for cryo-EM structure determination [132]. Images reproduced with permission from the following references: [123, 131, 132] Copyright 2007, 2012, 2016: NAS; [124, 125] Copyright 2013, 2011: NPG; [127] Copyright 2011: ACS.

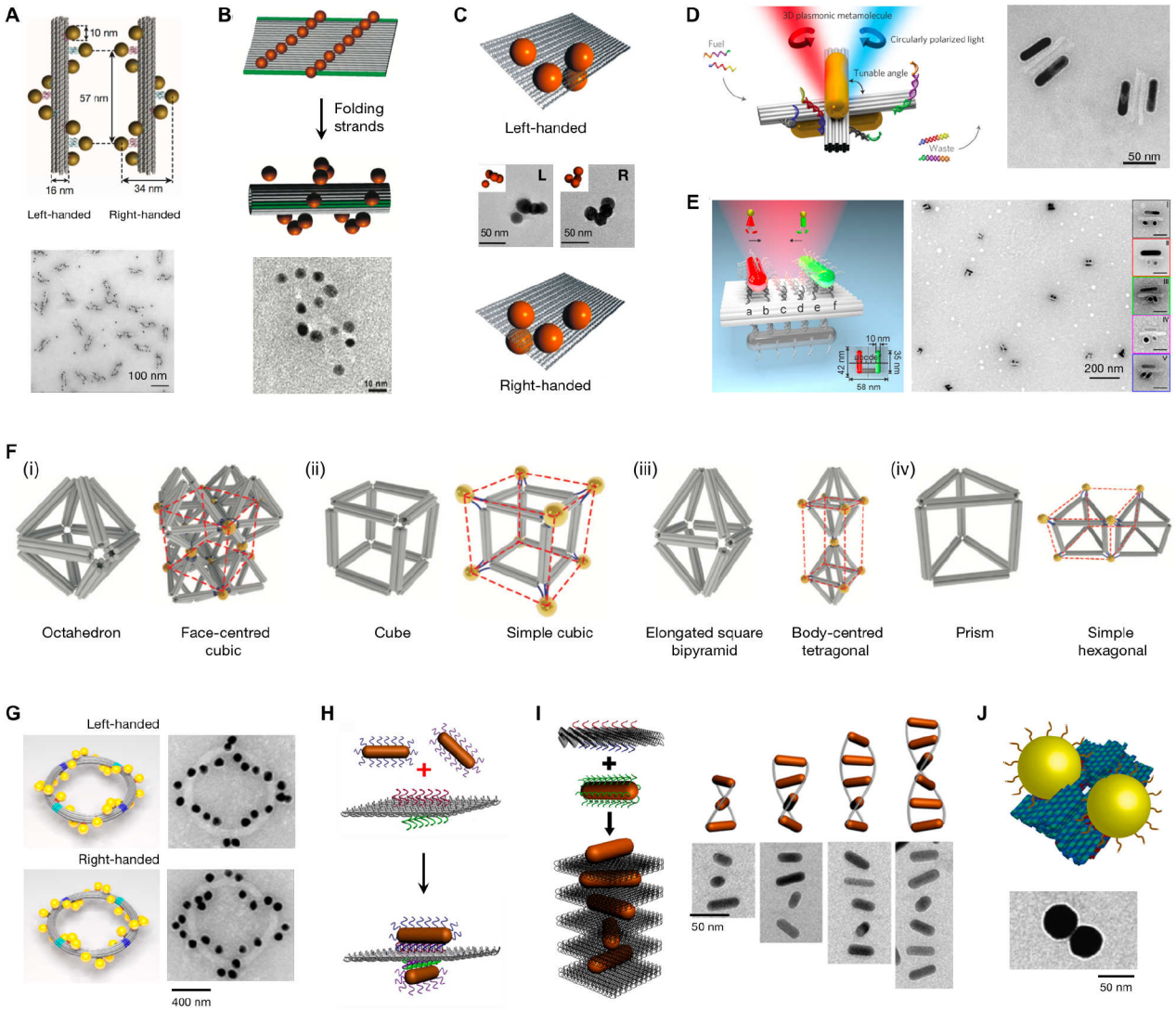

Figure 11. *DNA-based plasmonic nanostructures.* (A) DNA origami bundles for chiral arrangement of AuNPs [142] (B) DNA origami sheets with AuNPs rolled into chiral gold arrangements [143]. (C) Chiral tetramers arranged on DNA origami sheets [144] (D) Reconfigurable DNA plasmonic nanorods hosted on DNA origami device [145] (E) A nanoplasmonic walker on DNA origami [147]. (F) DNA origami frames used to create nanoparticle clusters. Frame shapes are shown on the left and the corresponding unit cells are shown on the right [148]. (G) Plasmonic toroidal metamolecules assembled by DNA origami [151]. (H) Gold nanorods with tunable position on DNA origami template [153]. (I) Gold nanorod helical superstructures with designed chirality arranged using DNA origami [154]. (J) DNA origami based assembly of gold nanoparticle dimers for surface-enhanced Raman scattering [155]. Images reproduced with permission from the following references: [142, 145, 148, 155] Copyright 2012, 2014, 2016, 2014: NPG; [143, 144, 147, 151, 153, 154] Copyright 2012, 2013, 2015, 2016, 2013, 2015: ACS.

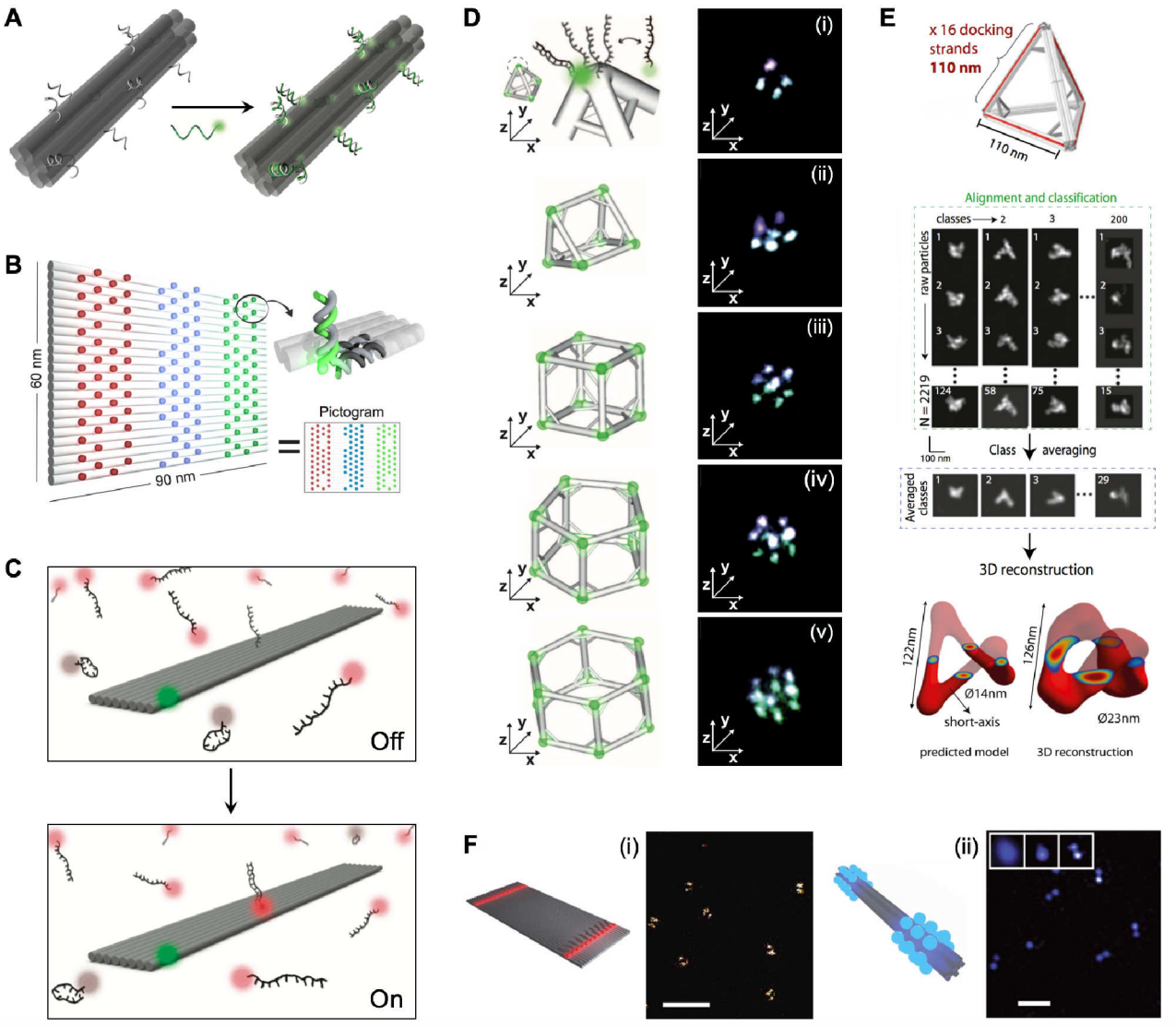

Figure 12. *DNA nanostructures for fluorescence imaging.* (A) Fluorescent barcode based on a DNA nanorods [172]. (B) DNA-based metafluorophores for patterned pictograms [173]. (C) Fluorescence imaging of transient binding on DNA origami for super-resolution microscopy [177]. (D) DNA origami polyhedra characterized by DNA-PAINT [60]. (E) 3D reconstruction of an origami tetrahedron structure from super-resolution light-microscopy images [183]. (F) DNA origami-based standards for quantitative fluorescence microscopy [186]. Images reproduced with permission from the following references: [172, 186] Copyright 2012, 2014: NPG; [60] Copyright 2014: AAAS; [177] Copyright 2010: ACS; [183] Copyright 2017: NAS.

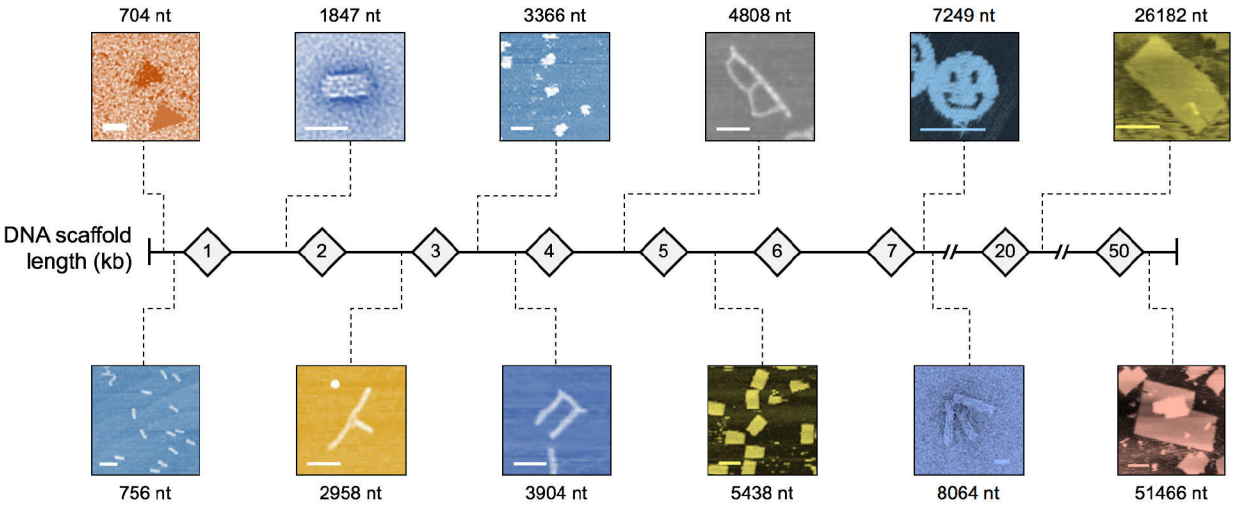

Figure 13. *Variations in DNA origami scaffolds.* The illustration shows different DNA origami structures constructed from single stranded scaffolds of different length (show in kilo bases). Scale bars represent 100 nm in AFM images and 20 nm in TEM images. AFM and TEM images reproduced with permission from references [52] Copyright 2006: NPG; [238, 242] Copyright 2009, 2014 respectively: ACS; [239, 240] Copyright 2012, 2013: RSC; [241] Copyright 2014 WILEY-VCH; [60] Copyright 2014: AAAS.

1 **Table 1. Protein/peptide components in DNA-based nanoscale constructs**

Protein component	DNA nanostructure	Binding route	Biophysical study/ Application/ Significance	Reference
Streptavidin	Nanowires, 2D arrays (cross motif), 2D origami	Biotin-avidin	Surface patterning, single molecule chemical reactions, sensors	313-315
Glucose oxidase/ horseradish peroxidase	DNA origami nanotube	Neutravidin-biotin	Molecular enzyme cascades	306
Zinc-finger protein	2D origami	DNA sequence recognition	As protein-binding adaptors	316
Cyan fluorescent protein, yellow fluorescent protein	2D origami	Sequence specific zinc-finger adaptors	Site-specific binding on DNA-origami	316
Platelet-derived growth factor	2D origami	Aptamer-binding	Protein array on origami, sensing	317
Thrombin	2D origami	Aptamer-binding	Protein array on origami, analysis of distant-dependent protein binding	317
RuvAB, Neurotensin receptor type 1 (NTS1), Guanine nucleotide binding protein (Gαi1)	2D Kagome-array formed from 4-arm junctions	Holliday junction-binding	Cryo-EM molecular support	126,127
Transthyretin	20-helix bundle origami nanotubes	DNA-peptide amide linkage	Amyloid nucleation and growth	318
Kinesin-1 Dyenin	6-helix bundle origami	SNAP tag, DNA-DNA	Biomimetic study of molecular motors	178
Enhanced yellow fluorescent protein (eYFP)	12-helix bundle origami	DNA-peptide amide linkage	Super-resolution microscopy	319
TATA box binding protein	Origami force clamp	DNA-binding	Measuring forces involving in protein binding	121
Green fluorescent protein	Origami device	Chemical conjugation	Analysis of biomolecular interactions based on nanoactuation	320
Nucleosomes	Origami nanocaliper/hinge	DNA-binding	Force spectrometers to study histone protein binding to DNA	115,116
Transcription factor p53	3D origami cage	Sequence-specific dsDNA binding	Molecular support in cryo-EM; structure solved at 14 Å	132
DegP (serine protease)	3D origami cage	DNA-peptide amide linkage; DNA-DNA	Multiple anchor stabilization of a 500 kDa protein in origami cage	323
eYFP, mKate, cytochrome C peroxidase (CCP), esterase 2 (EST2)	2D origami templates	Snap-tags and Halo-tags	Site-specific functionalization of nanostructures	321
RecA	Origami wireframe objects	DNA-binding	DNA-protein filament assembly	322
Engineered Drosophila Engrailed homeodomain (ENH)	Protein-mediated DNA nanowires	dsDNA-binding	DNA-protein hybrid nanoshapes; hierarchical assembly	78
Engineered transcription activator–like (TAL) effector Proteins	Protein-mediated dsDNA origami	dsDNA-binding	Programmable protein-mediated folding of dsDNA, DNA-protein hybrid nanoscale shapes	79

2